

## Article

# Rubber Degrading Strains: *Microtetraspora* and *Dactylosporangium*

Ann Anni Basik<sup>1,2</sup>, Jayaram Nanthini<sup>3</sup>, Tiong Chia Yeo<sup>2</sup> and Kumar Sudesh<sup>1,\*</sup> 

<sup>1</sup> Ecobiomaterial Research Laboratory, School of Biological Sciences, Universiti Sains Malaysia, George Town 11800, Malaysia; annbasik@sbc.org.my

<sup>2</sup> Sarawak Biodiversity Centre, Km. 20 Jalan Borneo Heights, Kuching 93250, Malaysia; cyeo@sbc.org.my

<sup>3</sup> Faculty of Arts & Science, School of Science & Psychology, International University of Malaya-Wales, Kuala Lumpur 50480, Malaysia; nanthini.jayaram@iumw.edu.my

\* Correspondence: ksudesh@usm.my; Tel.: +60-4-6534367; Fax: +60-4-6565125

**Abstract:** Rubber composed of highly unsaturated hydrocarbons, modified through addition of chemicals and vulcanization are widely used to date. However, the usage of rubber, faces many obstacles. These elastomeric materials are difficult to be re-used and recovered, leading to high post-consumer waste and vast environmental problems. Tyres, the major rubber waste source can take up to 80 years to naturally degrade. Experiments show that the latex clearing proteins (Lcp) found in Actinobacteria were reportedly critical for the initial oxidative cleavage of poly(*cis*-1,4-isoprene), the major polymeric unit of rubber. Although, more than 100 rubber degrading strains have been reported, only 8 Lcp proteins isolated from *Nocardia* (3), *Gordonia* (2), *Streptomyces* (1), *Rhodococcus* (1), and *Solimonas* (1) have been purified and biochemically characterized. Previous studies on rubber degrading strains and Lcp enzymes, implied that they are distinct. Following this, we aim to discover additional rubber degrading strains by randomly screening 940 Actinobacterial strains isolated from various locations in Sarawak on natural rubber (NR) latex agar. A total of 18 strains from 5 genera produced clearing zones on NR latex agar, and genes encoding Lcp were identified. We report here lcp genes from *Microtetraspora* sp. AC03309 (*lcp1* and *lcp2*) and *Dactylosporangium* sp. AC04546 (*lcp1*, *lcp2*, *lcp3*), together with the predicted genes related to rubber degradation. In silico analysis suggested that *Microtetraspora* sp. AC03309 is a distinct species closely related to *Microtetraspora glauca* while *Dactylosporangium* sp. AC04546 is a species closely related to *Dactylosporangium sucinum*. Genome-based characterization allowed the establishment of the strains taxonomic position and provided insights into their metabolic potential especially in biodegradation of rubber. Morphological changes and the spectrophotometric detection of aldehyde and keto groups indicated the degradation of the original material in rubber samples incubated with the strains. This confirms the strains' ability to utilize different rubber materials (fresh latex, NR product and vulcanized rubber) as the sole carbon source. Both strains exhibited different levels of biodegradation ability. Findings on tyre utilization capability by *Dactylosporangium* sp. AC04546 is of interest. The final aim is to find sustainable rubber treatment methods to treat rubber wastes.

**Keywords:** biodegradation; *Dactylosporangium*; genome; latex clearing protein; *Microtetraspora*



**Citation:** Basik, A.A.; Nanthini, J.; Yeo, T.C.; Sudesh, K. Rubber Degrading Strains: *Microtetraspora* and *Dactylosporangium*. *Polymers* **2021**, *13*, 3524. <https://doi.org/10.3390/polym13203524>

Academic Editors: Huihuang Ding and Qingbin Guo

Received: 9 September 2021

Accepted: 6 October 2021

Published: 13 October 2021

**Publisher's Note:** MDPI stays neutral with regard to jurisdictional claims in published maps and institutional affiliations.



**Copyright:** © 2021 by the authors. Licensee MDPI, Basel, Switzerland. This article is an open access article distributed under the terms and conditions of the Creative Commons Attribution (CC BY) license (<https://creativecommons.org/licenses/by/4.0/>).

## 1. Introduction

There is a great interest in developing environmentally sustainable methods to solve the rubber waste problem globally. Rubber consisting of poly(*cis*-1,4-isoprene) or poly(*trans*-1,4-isoprene) are highly modified through compounding and vulcanization in industrial processes and are used in more than 50,000 products today [1,2]. Rubber materials are resistant to thermal and chemical degradation. They are also difficult to re-use or recycle. And the majority of them are just discarded in landfills [3–5]. Robust, economical, and easily scalable methods for converting rubber products or waste into by-products or composites that ideally can be reused are desperately needed.

Rubber-degrading enzymes, produced by microbes, are a key discovery for biological rubber degradation. They consist of latex clearing protein (Lcp), mainly present in Actinobacteria and rubber oxygenases (RoxA and RoxB) found in Gram negative rubber degraders. There are 2 groups of rubber-degrading bacteria: (i) strains that produce clear zones on NR latex agar and (ii) strains that require direct contact with rubber substrates for subsequent degradation [6–8]. In both cases, enzymes produced by the bacteria extracellularly cleave rubber polymers containing hydrocarbon with a molecular weight (Mw) of  $10^5$  to  $10^6$  into mixtures of low Mw products  $C_{20}$ ,  $C_{25}$ ,  $C_{30}$  and higher oligo-isoprenoids as end products [9–11]. Oligomers with an Mw higher than 2000 were slowly degraded by microbes, while short oligomers of roughly 1000 Mw were rapidly consumed by the organism [12].

Actinobacteria are an integral part of the indigenous soil microflora, unique for their ability to degrade a large variety of organic materials, their high catabolic capacity, and their resilience in the face of unfavorable environmental conditions [13,14]. The same species of Actinobacteria growing in different locations or ecological niches are known to produce environmentally specific metabolites [15,16]. Biodiversity in Sarawak is a great advantage in our field of study. Actinobacteria that have evolved genes encoding catabolic enzymes that are functionally capable of degrading modified rubber are a potential solution for the end-of-life management of rubber products [4,17,18].

Our present survey of the Sarawak Biodiversity Centre (SBC) (<https://www.sbc.org.my/>, accessed on 5 June 2021) Actinobacteria Culture Collection is geared towards discovering novel rubber-degrading Actinobacteria. Most rubber-degrading strains discovered to date belong to the phylum, Actinobacteria (mainly *Streptomyces*, *Gordonia*, *Nocardia* and *Rhodococcus*) and are rarely found among Gram-negative bacteria and fungi [4,19–21]. Furthermore, several findings proved that different rubber-degrading strains possess different rubber-degrading ability. *Nocardia* genus, in particular *Nocardia nova* SH22a, has been characterized for its ability to degrade both poly(*cis*-1,4-isoprene) and poly(*trans*-1,4-isoprene) rubber [22,23]. The biochemical study of Lcp from *Rhodococcus rhodocrous* RPK1 showed substantial differences in its active site compared to Lcp of *Streptomyces* sp. K30 and *Gordonia polyisoprenivorans* VH2 [24]. In addition to that, a combination of different rubber oxygenases (RoxA/RoxB/Lcp) had a synergistic effect on rubber degradation [9]. The degradation rate of rubber products was also greatly improved when utilizing a consortium of rubber-degrading strains instead of using a specific strain [25,26]. To augment existing information and evaluate the diverse activities in these groups of bacteria, findings, and the characterization of new rubber degraders and their metabolic capacity, are required.

To date, a total of 248 lcp genes have been deposited into GenBank. This screening program led to the discovery of 2 new rubber-degrading genera, *Microtetrastora* and *Dactylosporangium* containing rubber-degrading genes. Limited information is available for both genera due their low isolation frequency. Classified as “rare Actinobacteria” only 22 and 16 Type strains have been published to date for *Microtetrastora* and *Dactylosporangium*, respectively [27]. There have been no reports on the biodegradation ability of *Microtetrastora* and *Dactylosporangium*, and their genome-based characterization as rubber degraders.

## 2. Materials and Methods

This research was carried out by firstly detecting rubber-degrading strains by screening them on natural rubber (NR) latex agar. Clear zone formation on NR latex agar indicated the ability of the strain to utilize NR latex. These strains were then morphologically and molecularly characterized. Based on the strain taxonomic and latex-clearing protein (lcp) genes characterization information, strains of interests of *Microtetrastora* sp. AC03309 and *Dactylosporangium* sp. AC04546 were selected for further studies. In silico studies of their genome through genomic sequencing were used to determine the strains’ novelty (taxonomic position, rubber-degrading genes and specialty genes). Both strains were also tested for their ability to utilize NR and vulcanized rubber (VR) as the sole carbon and energy source. The research approach flow chart is depicted in Supplementary Figure S1.

### 2.1. Screening for Clear Zone Forming Strains on Natural Rubber (NR) Latex Agar

Natural rubber (NR) latex agar preparation: the NR Latex agar preparation was modified from Braaz et al., 2004. [28] Mineral Salts Medium (MSM) per litre [ $K_2HPO_4$ , 8.0 g;  $KH_2PO_4$ , 1.0 g;  $(NH_4)_2SO_4$ , 0.5 g;  $MgSO_4 \cdot 7H_2O$ , 0.2 g; NaCl, 0.1 g;  $Ca(NO_3)_2$ , 0.1 g; 15 g agar] were added with 0.02% (v/v) NR latex concentrate and was sterilized by autoclaving for 15 min at 121 °C, 15 psi. After sterilization, 1 mL of 100× trace element solution was added.

NR latex concentrate: Crude rubber latex consists of 6% non-rubber constituents, mainly protein. High speed centrifugation was used to remove protein from freshly collected rubber latex. Fresh latex was transferred into high-speed polycarbonate centrifuge tube and equal volume of 0.002 % (v/v) Tween 80 was added, mixed well and then separated by centrifugation (5 min at 19,320× g). This washing step was repeated. The top layer or NR latex concentrate was removed and used to prepare the NR latex agar [29].

Trace elements (100×) per 100 mL [containing  $CaCl_2 \cdot 2H_2O$ , 0.2 g;  $FeSO_4 \cdot 7H_2O$ , 0.2 g;  $Na_2MoO_4 \cdot H_2O$ , 5 mg; and  $MnSO_4$ , 5 mg] were filter-sterilized [30].

MSM agar with NR latex concentrate were then transferred into 6-well plates (4 mL per well). Actinobacterial cultures cultivated in Yeast Malt Extract (ISP2) broth [31] for 3 to 14 days were spotted (40 µL) onto each agar well. The plates were incubated at 28 °C for up to 4 weeks. Colonies that produced translucent clearing zones, indicating the degradation of the NR latex, were recorded.

### 2.2. Identification of Clear Zone Forming Strains on Natural Rubber (NR) Latex Agar

Strains producing clear zones were taxonomically identified based on their morphological features and molecular techniques. Strains that were cultivated in ISP2 agar plate were used to capture and describe their morphology. Strains that were cultivated on Soil Extract agar (SEA) were used to observe the strains spore-forming structures [32]. SEA agar promotes the strains formation of spores and are translucent, easy for direct observation using a 50× long distance (Olympus LMPLFLN, Tokyo, Japan). Molecular identification was made based on the amplification of the 16S rDNA gene using primer 27F (5'-AGAGTTTGATCMTGGCTCAG-3') and 1492R (5'-TACGGYTACCTTGTTACGACTT-3') with the following parameters: 5 min at 96 °C, 30 cycles of 45 s at 96 °C, 2 min at 55 °C, 4 min at 72 °C and the final extension for 7 min at 72 °C. The amplified products were sent to Apical Scientific Sdn. Bhd., Selangor, Malaysia for sequencing. Sequence quality was checked using Sequence scanner version 2.0 (Applied Biosystems, Waltham, MA, United States) [33] and assembled by manual alignment (cap contig) using BioEdit software version 7.0.5.3 (North Carolina State University, Raleigh, NC, USA) [34]. The sequences were subjected to online BLASTN analysis against the 16S ribosomal RNA sequences (Bacteria and Archaea). Phylogenetic tree was generated using MEGA X software (Penn State University, State College, PA, USA) [35].

### 2.3. Profiling of Latex Clearing Protein (Lcp) Genes

The presence of lcp genes in the strains that produced clearing zones on NR agar were screened and amplified using the following primers: lcp441f [5'-GGAG(TG)C(GC)GC(GC)GTCTACTACTC-3'] and lcp879r [5'-GATCGG(AG)T(TC)GAG(AGC)ACCTGC-3'] [30], lcp1f [5'-ATGGAGAATCTCAGTAGACGT-3'] and lcp1199r [5'-ATGACCGGAATGGTGATCGG-3'], designed based on the conserved regions of published lcp gene sequences (*Micromonospora* sp. WMMB235 (ENA accession number MDRX01000001), *Micromonospora* sp. TSRI0369 (ENA accession number LIVU01000002), *Micromonospora* sp. NRRL B-16802 (ENA accession number NZLGEB01000064), *Micromonospora echinospora* ATCC15837 (ENA accession number NGNT01000005). The target genes were amplified using the following parameters: 2 min at 95 °C, 30 cycles of 30 s at 95 °C, 1 min at 55–65 °C, 2 min at 72 °C and the final extension for 5 min at 72 °C. Annealing temperature was optimized for each strain.

Amplified products were sent to Apical Scientific Sdn. Bhd., Selangor, Malaysia for sequencing. Sequence quality was checked using a Sequence scanner version 2.0

(Applied Biosystems, Waltham, MA, USA) [33] and assembled by manual alignment (cap contig) using BioEdit software version 7.0.5.3 (North Carolina State University, Raleigh, NC, USA) [34]. The sequence's blast homology was compared to the UniProt database [36]. Nucleotide sequences were translated into amino acids using ExPASy (SIB Swiss Institute of Bioinformatics, Lausanne, Switzerland) [37] to identify the open reading frame (ORF). ORF were subjected to BlastP (GenBank, MD, USA) to obtain Protein Blast homology.

#### 2.4. Genomic Deoxyribonucleic Acid (DNA) Isolation

Genomic DNA (gDNA) for *Microtetraspora* sp. AC03309 and *Dactylosporangium* sp. AC04546 were extracted and purified using an adapted method from Moore et al., (2008) [38]. Strains were first cultivated in 20 mL ISP2 broth in a 250 mL flask at 28 °C, 180 rpm for 7 to 10 days. Harvested Actinobacterial cells were centrifuged and washed with sterile water twice to remove any growth media. The cells (~0.1 g) in PCR tubes were then resuspended in 550 µL 1xTris-EDTA buffer and mixed well. Lysozyme (for cell lysis) with final concentration of 2 mg mL<sup>-1</sup> and 5 µL Rnase A solution (10 mg mL<sup>-1</sup>) were added and incubated at 37 °C for 90 min. Then 10% (v/v) SDS (final concentration 1% v/v) and Proteinase K 10 mg mL<sup>-1</sup> (final concentration 1 mg mL<sup>-1</sup>) were added and incubated at 65 °C for 90 min. SDS is an anionic detergent which binds cellular proteins and lipoproteins, effectively denaturing them and promoting the dissociation of nucleic acids. 5M NaCl was added (final concentration 0.7 M) and incubated at 65 °C for 2 min, then pre-warmed CTAB (hexadecyltrimethylammonium bromide) (final concentration 1% v/v) was added and incubated at 65 °C for another 10 min. CTAB has also been proven useful for DNA extractions from bacterial cells by denaturing and precipitating the cell wall lipopolysaccharides and proteins. In the presence of monovalent cation (e.g., Na<sup>+</sup>) concentrations above 0.5 M, DNA will remain soluble.

To purify the gDNA sample, equal volume (v/v) of CIA (24: 1, chloroform: isoamyl alcohol) was added, inverted to mix, and centrifuge at 10,000 rpm for 5 min. This step was repeated twice. The top layer was transferred and added with equal volume of isopropanol. The sample is kept at -20 °C overnight to allow gDNA to precipitate. Genomic DNA was pellet by centrifuging at 14,000 rpm for 15 min. Isopropanol was removed, and the gDNA pellet washed with 70% molecular grade ethanol. Genomic DNA was pellet by centrifuging at 14,000 rpm for 15 min. Ethanol was discarded and the tube containing gDNA pellet was left to air dry. Finally, the gDNA was resuspended in 10 mM Tris-HCL buffer pH8.5. DNA quantity and quality was checked using BioSpectrophotometer (Eppendorf AG, Germany).

Genomic DNA was then analyzed for its integrity and purity using gel electrophoresis. A minimum amount of 200 ng gDNA eluted in 30 µL Tris-HCl buffer (DNA concentration 6 µg) was required for library preparation (Nextera XT Library Prep Kit, Illumina, CA, USA) prior to sequencing. The purified DNA samples were subsequently sent for genomic sequencing using Illumina MiSeq sequencer (Illumina, CA, USA) and were assembled (SPAdes) by service provider BioEasy Sdn. Bhd., Selangor, Malaysia.

Genomic DNA extraction was also carried out for all the clear zone forming strains for 16S rRNA and latex-clearing protein (lcp) gene amplification using polymerase chain reaction (PCR).

#### 2.5. Genome Attributes and Annotation

Draft genome for *Microtetraspora* sp. AC03309 and *Dactylosporangium* sp. AC04546 were annotated using RAST server version 2.0 [39], PATRIC server version 3.6.12 [40] and NCBI Prokaryotic Genome Annotation Pipeline (PGAP) [41]. Gene function annotation for Clusters of Orthologous Groups (COGs) were carried out using egg-NOG mapper v.2 [42]. COG retain the same function and are orthologous across at least three lineages, likely corresponds to an ancient, conserved domain [43]. To determine the related genes/protein and location in a pathway, the KEGG Pathway database was used [44]. Clustered regularly interspaced short palindromic repeats (CRISPRs) were used to depict the genome readability for bacteriophage exposure and genome-editing [45]. To predict the antibiotic-

resistant genes, antibiotic-resistant homologs search was carried out in the CARD database (<https://card.mcmaster.ca/analyze/rgi>, accessed on 5 June 2021) [46]. Drug targets were identified using PARTIC server [40] and verified using DrugBank 5.0 [47].

The strains' ability to produce secondary metabolites was predicted using The Antibiotics and Secondary Metabolite Analysis Shell (AntiSMASH) 6.0 software [48].

To determine the location of protein-coding genes (CDS) and open reading frame (ORF) on the draft genome, sequence contigs were viewed using The SEED Viewer [49] and SnapGene Viewer (<https://www.snapgene.com/>, accessed on 5 March 2020).

CDS and amino acid sequence for latex clearing protein (Lcp), 1-oxidoreductase beta subunit (oxiB) and 1-oxidoreductase alpha subunit (oxiA) were verified through the presence of ribosome-binding site (RBS), and comparison with sequences in UniProt [50] and GenBank database. The prediction of twin arginine translocation (Tat) signal peptides was carried out using TatP 1.0 server (Department of Health and Technology, Lyngby, Denmark) [51]. ExPASy was used to determine the predicted protein molecular weight (Mw) and their theoretical isoelectric point (pI) [37].

## 2.6. Taxonomic Delineation

The taxonomic position of *Microtetraspora* sp. AC03309 and *Dactylosporangium* sp. AC04546 was determined using polyphasic approaches, including (i) 16S rRNA gene-based method, (ii) average nucleotide identity (ANI) using FastANI (KBase Software, U.S. Department of Energy, Washington, DC, USA) [52], (iii) in silico DNA-DNA hybridization (dDDH) estimate method and (iv) genome relatedness and phylogenetic analysis. Both dDDH and phylogenetic analysis (16S rRNA and genome) was conducted using Type (Strain) Genome Server (TYGS) (DSMZ, Braunschweig, Germany) [53]. A minimum of 20% of the genome is required to obtain the same result as the full genome [54]. Better-resolved phylogenies, based on the hundreds of housekeeping genes or even the core-genome, has been used to elucidate the phylogenetic relationships classifications based on whole genome sequences [55].

## 2.7. Utilization of Rubber Materials

To study the ability of *Microtetraspora* sp. AC03309 and *Dactylosporangium* sp. AC04546 in utilizing different rubber materials as the sole carbon and energy source; fresh latex, rubber gloves and tyres samples were used. Fresh latex was harvested from 5-year-old rubber trees at a rubber plantation site at Kulim, Kedah, Malaysia. The latex was brought back and left to solidify at room temperature. Solid latex pieces were then cut into ~1.0 cm × 1.0 cm pieces. Steel-free tyre granules (1.0 to 3.0 mm) were obtained from a tyre recycling factory (Gcycle Tyre Recycling) in Bedong, Kedah, Malaysia. Latex gloves (PRO-CARE), disposable and non-powdered, were used in these studies. Latex gloves were cut into strips of ~0.5 cm × 1.0 cm.

For short-term evaluation under laboratory conditions, antimicrobial substances from the latex glove and tyre granules were removed prior to cultivation. The rubber materials were treated with chloroform as follows: 1 g of sample with 100 mL for 12 h. During this period the solvent was replaced one to two times with fresh chloroform. The treated material was left to air dry; then, it was sterilized by autoclaving and subsequently used as carbon source [56]. No changes in the surface (cracks and holes) of the rubber material were observed using Scanning Electron Microscope (SEM) (Quanta FEG 650, Thermo Fisher Scientific, Edinburgh, UK) before and after chloroform treatment.

Pre-culture of actively growing strains were cultivated in ISP2 broth. The culture (1 mL) were transferred into 250 mL test flasks containing 50 mL MSM and 0.5% (*w/v*) rubber material [56]. The inoculated flasks were then incubated at 28 °C, 180 rpm for 30 days. Test flasks without culture were used as control. All the sample studied were carried out in triplicates.

- Morphological Observation using Scanning Electron Microscope (SEM)

Inoculated rubber samples were harvested and air-dried for direct observation. To observe the surface of the tested rubber material, the strain biofilm and mycelia on the rubber particles were removed by rinsing the rubber materials with distilled water. Then, immersing them in 96% ethanol (Sigma-Aldrich, Switzerland) for 1 h before air-drying at ambient temperature. Both washed and unwashed samples were prepared using the hexamethyldisilazane (HDMS, Sigma-Aldrich, Switzerland) method prior to SEM viewing. Samples were placed into shell vials (1.8 mL) and fixed by immersing it in *McDowell-Trump* fixative (Thermo Fisher Scientific, Waltham, MA, USA) solution, prepared in 0.1 M phosphate buffer (pH 7.2) (Sigma-Aldrich, Switzerland) at 4 °C for at least 2 h. The samples were then washed in 0.1 M phosphate buffer (pH 7.2) (Sigma-Aldrich, Switzerland) for 10 min, this step is repeated twice. Samples were post-fixed by immersing them in 1% (*v/v*) osmium tetroxide prepared in 0.1 M phosphate buffer (Sigma-Aldrich, Switzerland) (pH 7.2) for 1 h. This step was carried out in the chemical hood. Then the samples were washed by immersing them in distilled water for 10 min. This step was repeated twice. Dehydration of the samples was carried out using ethanol. Firstly, the samples were immersed in 50% ethanol (Sigma-Aldrich, Switzerland) for 15 min, followed by 75% for 15 min, 95% for 15 min (twice) and finally 100% for 20 min (3 times). The dehydrated samples were then immersed in 1 mL HDMS for 10 min. HDMS acts as a drying agent. HDMS solutions were discarded, and the samples were left to dry in the desiccator. The dried samples were then mounted onto an SEM stub using double tape, coated with gold using Quorum Q150T S sputter coater (Quorum Technologies Ltd., East Sussex, UK) for observation using SEM Quanta FEG 650 (Thermo Fisher Scientific, Edinburgh, UK).

- Attenuated Total Reflection-Fourier Transform Infrared (ATR-FTIR)

Strain biofilm and mycelia were removed from the tested rubber samples by rinsing them with distilled water. Samples were then immersed in 96% ethanol for 1 h before air-drying them at room temperature. FTIR-ATR was used to determine the formation of new, or disappearance of functional groups in the polymer units of the samples by observing the presence, increase and decrease in C=C, C-C and C-H bonds. Post-incubation samples (fresh latex, latex glove, tyre) and non-inoculated samples were analyzed using ATR-FTIR Spectrum 400 (Perkim Elmer), equipped with ATR ranging from 4000  $\text{cm}^{-1}$  to 650  $\text{cm}^{-1}$ , with 4  $\text{cm}^{-1}$  resolution.

### 3. Results

#### 3.1. Screening for Clear Zone Forming Strains on Natural Rubber (NR) Latex Agar

Since 2006, Sarawak Biodiversity Centre (SBC) has been collecting environmental samples from various locations across Sarawak in efforts to isolate microbes mainly Actinobacteria and fungi as part of their inventory. To evaluate the potential application of the Actinobacterial Culture Collection as rubber degraders, a total of 940 strains were randomly selected and screened on NR latex agar. The strains tested consisted of Actinobacteria from 9 families (15 genera) and 205 Actinobacteria strains that could not be classified based on morphology (Table 1). Eighteen (18) strains were found to be capable of degrading NR latex, producing ~1 to 2 mm clearance surrounding the colony.

#### 3.2. Taxonomic Identification of Clear Zone Forming Strains

All of the 18 strains producing clear zones were successfully identified through PCR amplification of their 16S rDNA gene having blast homology ranging from 99.00 to 100.00% (MT005091, MT005089, MT005088, MT005098, MT005101, MT005095, MT005096, MT005104, MT005094, MT005105, MT005103, MT005100, MT005099, MT005102, MT005097, MT005093, MT005090, MT005092). Blast homology of 98.70–99.50% are putative novel species, 99.60–99.80% are putative known species and 99.90% and above are identical or closely related species [57].

**Table 1.** Screening of Sarawak Biodiversity Centre (SBC) Actinobacteria Culture Collection for rubber degraders.

| Family                 | Genera                   | No. of Strains Tested | Clear Zone Formation |
|------------------------|--------------------------|-----------------------|----------------------|
| Streptomycetaceae      | <i>Streptomyces</i>      | 526                   | 2                    |
|                        | <i>Kitasatospora</i>     | 12                    | 0                    |
| Micromonosporaceae     | <i>Micromonospora</i>    | 86                    | 6                    |
|                        | <i>Dactylosporangium</i> | 3                     | 1                    |
| Streptosporangiaceae   | <i>Nonomuraea</i>        | 31                    | 2                    |
|                        | <i>Microtetraspora</i>   | 11                    | 7                    |
|                        | <i>Microbispora</i>      | 4                     | 0                    |
|                        | <i>Herbidospira</i>      | 2                     | 0                    |
| Thermoactinomycetaceae | <i>Shimazuella</i>       | 1                     | 0                    |
| Thermomonosporaceae    | <i>Actinomadura</i>      | 8                     | 0                    |
|                        | <i>Actinoallomurus</i>   | 1                     | 0                    |
| Pseudonocardiaceae     | <i>Actinomycetospora</i> | 1                     | 0                    |
| Thermosporotrichaceae  | <i>Thermosporothrix</i>  | 1                     | 0                    |
| Mycobacteriaceae       | <i>Mycobacterium</i>     | 2                     | 0                    |
| Nocardiaceae           | <i>Nocardia</i>          | 46                    | 0                    |
|                        | Others                   | 205                   | 0                    |
|                        |                          | 940                   | 18                   |

Identification of the strains were based on the strain's morphology, spore-forming structures, some having 16S rRNA molecular information. Others: unable to determine genus based on morphology.

Clear zone forming strains were distributed among 5 genera: *Microtetraspora* sp. (7 strains), *Micromonospora* sp. (6 strains), *Streptomyces* sp. (2 strains), *Nonomuraea* sp. (2 strains) and *Dactylosporangium* sp. (1 strain). Although 39% of clear zone formers identified in this study belong to *Microtetraspora* genus, phylogenetic distribution of 16S rRNA gene suggests that they are not identical (Supplementary Figure S2).

### 3.3. Profiling of Latex Clearing Protein (Lcp) Genes in Clear Zone Forming Strains

Latex-clearing protein (Lcp) is responsible for the formation of clear zones on natural rubber (NR) overlay agar plates [58]. Blast homology of the amplified gene sequence was compared to the UniProt database, resulting in 81.20 to 100.00% blast identity to closely related proteins. The amplified nucleotide sequences were curated and submitted to GenBank with the following accession numbers: MN148090, MT241322, MN148093, MN148092, MN148094, MN148095, MT252675, MN148097, MN148098, MT241320, MN148096, MT241323, MT241319, MT241318, MT241317, MT252676, MT241321, MN148089.

Lcp amino acid sequences have been reported to contain 13-residues-long highly conserved region "KTRLVHAAVRHLL" [59]. ClustalW multiple alignment of the amplified Lcp amino acid sequences obtained in this study contained the highly conserved region, except for *Micromonospora* sp. AC03293 and *Streptomyces* sp. AC04842 (Supplementary Figure S3). Although the conserved region was not detected for strain *Micromonospora* sp. AC03293 due to its short sequence, the Lcp blast homology was 95.90% identity to *Micromonospora* sp. WMMB235 lcp gene. A comparison of Lcp amino acid sequence for *Micromonospora* sp. AC03293 and biochemically characterized Lcp from *Nocardia nova* SH22a also showed close similarity (85.70%). PCR amplification of *Streptomyces* sp. AC04842 lcp gene region was unsuccessful. Blast homology shows that it was 85.40% identical to a hypothetical protein of *Streptomyces* sp. 4F (QIS63111.1). However, in a separate study, we were able to identify lcp-homologues (MT664881 and MT664882) in the draft genome of *Streptomyces* sp. AC04842, containing the 13-residues-long highly conserved region.

### 3.4. Strain of Interest: *Microtetraspora* sp. AC03309 (JCM 34240)

The *lcp* gene and the genomic characterization for both genera, *Microtetraspora* and *Dactylosporangium* have not been reported. Therefore, we chose to further explore them through: (i) morphological studies and taxonomic delineation, (ii) prediction of genes related to rubber degradation through genome sequencing, and (iii) their ability to utilize different rubber products as the sole carbon and energy source.

*Microtetraspora* sp. AC03309 was isolated from a soil sample collected in a forest nearby Kampung Kiding, Padawan, Sarawak in 2006.

#### 3.4.1. Morphological Characterization of *Microtetraspora* sp. AC03309

Morphological characteristics of *Microtetraspora* sp. AC03309 can be seen in (Figure 1). *Microtetraspora* sp. AC03309 has blue green surface and honey gold reverse color on ISP2 agar with moderate aerial mycelia. Colony is wrinkled with regular shape; it has external short spore chains (approx. 3  $\mu\text{m}$  length) with 4 spores formed on sporophore branching from aerial hyphae. Spores are slightly oval to cylindrical with smooth surfaces. It grows well at 28  $^{\circ}\text{C}$ , with poor growth at 40  $^{\circ}\text{C}$  and 45  $^{\circ}\text{C}$  on ISP2 agar.

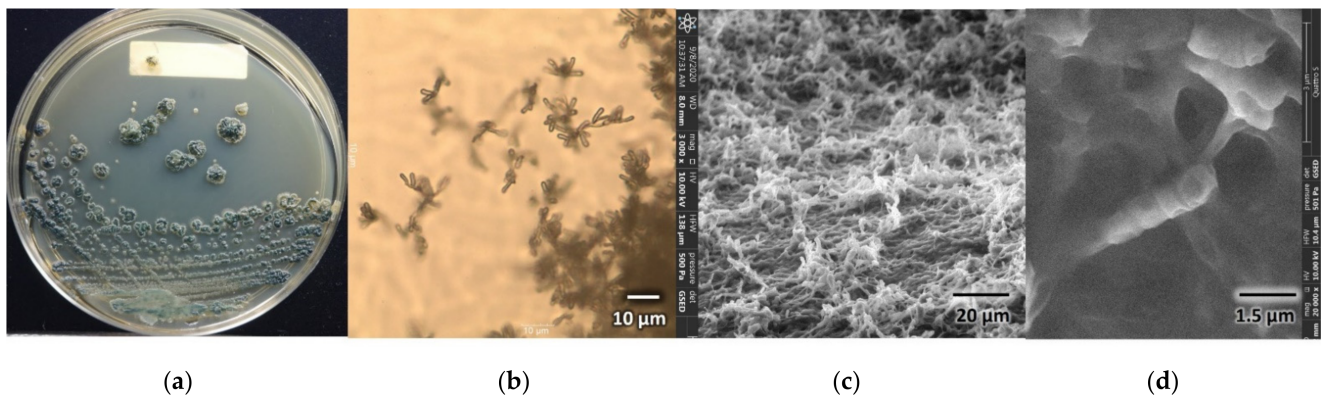


**Figure 1.** *Microtetraspora* sp. AC03309 morphology: (a) surface colony morphology on Yeast Malt Extract (ISP2) agar; (b) spore-forming structures viewed using light microscope at 750 $\times$  magnification on Soil Extract agar (SEA); (c) sporophore branching from aerial mycelia viewed using Field Emission Scanning Electron Microscope (FESEM, Quattro Thermo Fisher Scientific, Lanham, MD, USA); (d) sporophore with four spores viewed using Field Emission Scanning Electron Microscope (FESEM, Quattro Thermo Fisher Scientific, Lanham, MD, USA).

#### 3.4.2. *Microtetraspora* sp. AC03309 Taxonomic Delineation

The complete 16S rRNA gene sequence for *Microtetraspora* sp. AC03309 (1477 bp) was used for online BLASTN analysis against the 16S ribosomal RNA sequences (Bacteria and Archaea). *Microtetraspora* sp. AC03309 had a 98.85% identity to *Microtetraspora glauca* strain IFO 14761 (NR\_112346.1). The recommended threshold of >98.65% 16S rRNA gene sequence similarity is used as a threshold for differentiating two species [60].

Currently, bacterial species are defined as including strains that have 95.00–96.00% of average nucleotide identity (ANI) and 70.00% of digital DDH (dDDH) [61]. Analysis between *Microtetraspora* sp. AC03309 and *Microtetraspora glauca* draft genome (TYGS, <https://tygs.dsmz.de>, accessed on 25 June 2021) provided an ANI estimate of 97.33%, digital DNA-DNA hybridization (dDDH) of 77.00%, together with genome-based phylogeny predicts that they belong to the same species (Figure 2). However, dDDH value of less than 79.00% suggests *Microtetraspora* sp. AC03309 strain to be of a distinct subspecies [53].

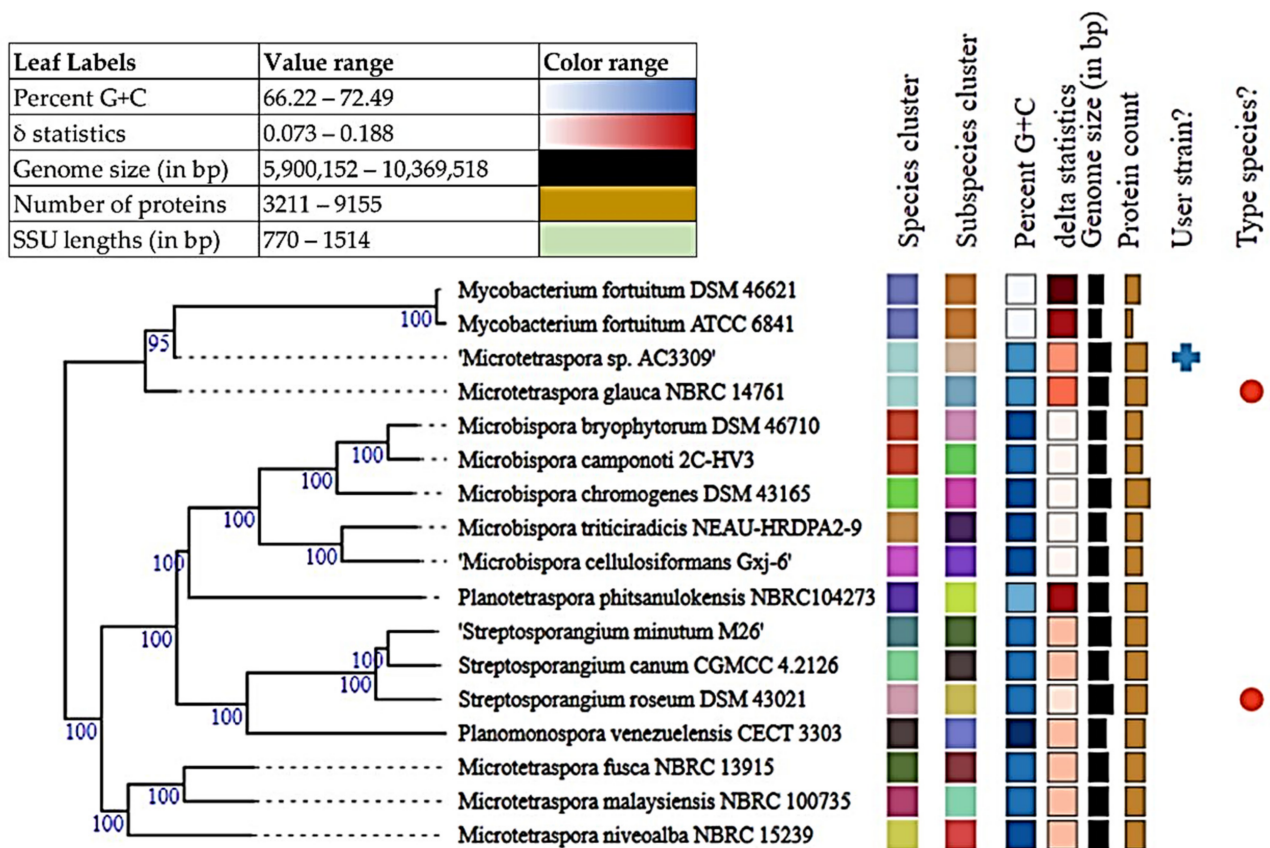


**Figure 2.** Tree inferred with FastME 2.1.6.1 (Lefort et al., 2015) from GBDP distances calculated from genome sequences. The branch lengths are scaled in terms of GBDP distance formula d5. The numbers above branches are GBDP pseudo-bootstrap support values > 60% from 100 replications, with an average branch support of 100%. The tree was rooted at the midpoint [62].

### 3.4.3. *Microtetraspora* sp. AC03309 Genomic Attributes

- Genomic & Protein Features

The draft genome for *Microtetraspora* sp. AC03309 (JADDIL000000000) has a size of almost 9.5 kb (9,434,728 bp) with a DNA G+C content of 71.0 mol%. The draft genome has a capacity for 8625 protein encoding genes as well as rRNAs [5S (2), 16S (2), 23S (3)] and 64 tRNAs. Subsystem coverage is 31% which contributes to a total of 461 subsystems out of 8625 CDS predicted by RAST server (Supplementary Figure S4). Predicted proteins were further analyzed into different functional classes based on Cluster of Orthologous Groups (COGs). Out of 7006 proteins, 4995 were mapped to unique COGs, which were further classified into metabolism (33.80%), cellular processes and signaling (16.16%), information storage and processing (20.77%) and poorly characterized (19.53%) functional classes. The remaining 9.75% proteins were assigned to more than one of the COGs categories and were grouped into Multiple COG (Figure A1, Appendix A). CRISPRFinder detected two confirmed CRISPR sites accessible for bacteriophage exposure and genome modification (Table A1, Appendix A).

- Specialty Genes:

Two antibiotic-resistant genes were predicted using CARD database (strict criteria), with functions in antibiotic resistance towards elfamycin (ARO: 3003361) and rapamycin antibiotic (ARO:3002883) (Table A2). A total of three drug targets were verified using DRUGBANK; 1 putative gene encoding Serine/threonine-protein kinase PknB, PknB [Pfam: Pkinase 379 (PF00069), PASTA (PF03793)], 1 putative gene encoding Recombinase A, RecA (Pfam: 380 PF00154), 1 putative gene encoding cell division protein FtsZ, ftsZ [Pfam: Tubulin 381 (PF00091) and FtsZ\_C (PF12327) [Pfam: ProteasomePF00227] (Table A3).

- Secondary Metabolite Clusters:

A total of 26 secondary metabolite biosynthetic gene clusters (BGCs) were predicted using AntiSMASH software (Table A4). Four BGCs showed more than a 50% similarity to known compounds (geosmin, desferrioxamine E, alkylresorcinol and catenulipectin), 13 BGCs with less than a 50% similarity to known compounds and 9 BGCs with no match. Interestingly, 2 BGCs of type I polyketide synthase (T1PKS) were detected, with BGCs of a 25% similarity to nostopeptolide A2 and a 40% similarity to labyrinthopeptin A2. T1PKS has been extensively studied and found in fungi, producing structurally diverse bioactive molecules, with very few found in bacteria [63].

- Sulfur Metabolism:

Desulfurization of vulcanized rubber is needed to reformulate and reuse rubber. Microorganism's ability to break the sulfur bonds (C-S) in vulcanized rubber would provide higher surface area for latex-clearing protein (Lcp) to cleave the polymer backbone chain during biodegradation. *Microtetraspora* sp. AC03309 draft genome contained genes encoding for inorganic and organic sulfur metabolism (KEGG pathway ko:00920 and ko:02010). A total of 76 putative genes for sulfur metabolism were detected, with 21 genes categorized under general sulfur metabolism, 28 genes under inorganic sulfur metabolism and 27 genes under organic sulfur metabolism. Most of the genes encode organic sulfur metabolism of alkanesulfonate and inorganic sulfur assimilation of sulfate/thiosulfate metabolism (Table A5).

#### 3.4.4. Identification of Latex Clearing Protein (Lcp) Homolog for *Microtetraspora* sp. AC03309

NCBI Conserved Domain Database (CDD) search, shows that *Microtetraspora* sp. AC03309 lcp-homologs (*lcp1* gene and *lcp2* gene) belongs to the DUF2236 domain-containing protein (accession pfam 09995) similar to latex-clearing protein (Lcp) for *Streptomyces* sp. K30. This is the first operon (*lcp-oxiAB*) structure reported for 2-lcp homolog located on the chromosome. *Microtetraspora* sp. AC03309 *lcp1* and *lcp2* genes were located adjacent to each other (Figure 3). Both lcp amino acid sequences showed a 58.50% similarity and contained the 13-residue long highly conserved region.

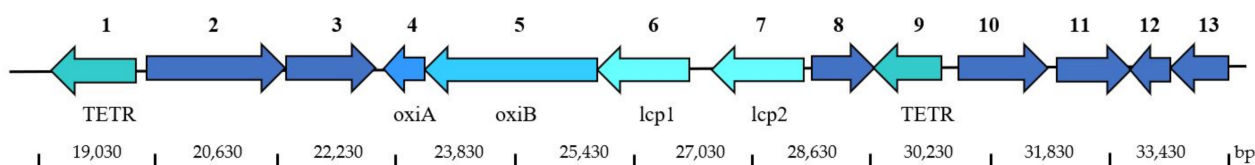


**Figure 3.** Location of *lcp1* and *lcp2*, and adjacent genes in *Microtetraspora* sp. AC03309 located on chromosome (contig 3): 1, Transcriptional regulator, TETR family; 2, Long chain fatty acid CoA ligase (EC 6.2.1.3); 3, Acetyl CoA dehydrogenase, short chain specific (EC 1.3.99.2); 4, Isoquinoline 1-oxidoreductase alpha subunit (*oxiA*); 5, Isoquinoline 1-oxidoreductase beta subunit (*oxiB*); 6, latex clearing protein 1 (*lcp1*); 7, latex clearing protein 2 (*lcp2*); 8, hypothetical protein; 9, Transcriptional regulator, TETR family; 10, MFS transporter; 11, hypothetical protein; 12, N-acetyltransferase; 13, pirin.

The *lcp1* gene (MW659698) is located on contig 3 at 26,812 to 25,649 bp. CDS translation results in 427 amino acids, encoding a protein with a theoretical mass of 47.0 kDa and 5.81 pI. Twin arginine translocation (TAT) signal peptide cleavage site was predicted between 30 and 31 bp (ARA-MP). Putative ribosomal site (RBS) was detected at 2 bp upstream from the putative start codon. The *lcp1* gene (1281 bp) showed 80.20% blast homology to latex clearing protein of *Actinophytocola xinjiangensis* (BLA60\_08475). *lcp1* amino acid sequence was 51.37% similar to characterized Lcp of *Gordonia polyisoprenivorans* VH2 (ABV68923.1).

The *lcp2* gene (MW659699) is located on contig 3 at 28,435 to 27,206 bp, 277 bp upstream of *lcp1* gene. CDS translation results in 410 amino acids, encoding a protein with a theoretical mass of 44.8 kDa and 6.55 pI. A twin arginine translocation (TAT) signal

peptide cleavage site was predicted between 30 and 31 bp (AQA-RT). A putative ribosomal site (RBS) was detected at 3 bp upstream from the putative start codon. The *lcp2* gene (1230 bp) showed 75.50% blast homology to latex-clearing protein of *Streptosporangium minutum* (A0A243RYB8\_9ACTN). Lcp1 amino acid sequence had a 63.66% similarity to characterized Lcp of *Gordonia polyisoprenivorans* VH2 (ABV68923.1).

#### 3.4.5. Predicted Genes Involved in Rubber Degradation for *Microtetraspora* sp. AC03309

The degradation pathway of rubber was proposed by the identification of intermediate metabolites and experimental studies based on the genomes for *Streptomyces coelicolor* 1A, *Nocardia* sp. 835A, *Steroidobacter cummioxidans* sp. nov., strain 35Y, *Gordonia polyisoprenivorans* VH2 and *Nocardia nova* SH22a [12,23,64–68]. Based on these findings, putative genes that participate in the rubber degradation in *Microtetraspora* sp. AC03309 were identified in its draft genome (Table A6).

TetR-family is a regulatory mechanism that induces the production of Lcp protein during metabolization of rubber [69–71]. A total of 152 TETR-family genes were found. Two TETR encoding genes located near the *lcp* genes could be involved in the Lcp transcription (Figure 3). One TETR encoding gene is located 118 bp downstream of *lcp2* and *lcp1*, and another was located upstream 1023 bp of *lcp1* and *lcp2*. Lcp is secreted outside the bacterial cell via twin-arginine translocation (TAT) pathway. Four putative gene coding TAT proteins were identified. The *oxiB* (MZ726746) and *oxiA* (MZ726747) gene located downstream of *lcp1* and *lcp2* gene is an oxidoreductase that converts the oligo-isoprenoid terminal aldehyde group to a carboxylic acid group. Isoprenoid acids are then transported into the bacterial cell through Mammalian cell entry (Mce). Two candidate genes of MCE-family protein were found. Resulting isoprenoid acids enter the  $\beta$ -oxidation cycle and are converted into acyl-CoA thioester by an acyl-CoA synthase (3 candidate genes). Acyl-CoA thioester are further catabolized by an acyl-CoA dehydrogenase (EC 1.3.8.1 & EC 1.3.8.7) (6 candidate genes). Polyunsaturated fatty acids degradation occur when 2,4-dienoyl-CoA reductase (EC 1.3.1.34) (1 candidate gene, NADH:flavin oxidoreductases, Old Yellow Enzyme family) catalyzes double bonds at the even-numbered position, followed by isomerization by enoyl-CoA hydratases (EC 4.2.1.17) (14 candidate genes). Six homologous genes for 3-hydroxyacyl-CoA dehydrogenases (EC 1.1.1.35) were identified, possibly involved in the following hydration step, responsible for the conversion of the hydroxyl derivatives into the keto. The last step of the first-oxidation cycle is predicted to be catalyzed by the thiolase/3-ketoacyl-CoA thiolase (EC 2.3.1.16) (6 candidate genes).

Mutants with a disruption of the  $\alpha$ -methylacyl-CoA racemase (*Mcr*) gene lost the ability to metabolize poly-(*cis*-1,4-isoprene) and related methyl-branched isoprenoid compounds (Arenskötter et al., 2008). Three *mcr* genes (EC 5.1.99.4) were also identified in the genome of *Microtetraspora* sp. AC03309.

In addition, 2 candidate genes for superoxide dismutase (*SodA*)(EC 1.15.1.1) were also identified, believed to serve as a radical scavenger during degradation of poly(*cis*-1,4-isoprene), as the formation of *SodA* is induced during growth on rubber [72].

The presence of these genes in the genome of *Microtetraspora* sp. AC03309 suggests that this genome may share the same rubber degradation pathway as predicted previously.

### 3.5. Strain of Interest: *Dactylosporangium* sp. AC04546 (JCM 34239)

*Dactylosporangium* sp. AC04546 was isolated from a soil sample in a forest collected at Lanchang, Serian, Sarawak in 2007.

#### 3.5.1. Morphological Characterization of *Dactylosporangium* sp. AC04546

Morphological characteristics of *Dactylosporangium* sp. AC04546 can be seen in Figure 4. *Dactylosporangium* sp. AC04546 has yellowish orange surface and reverse color on ISP2 agar with moderate aerial mycelia. Colony is wrinkled with regular shape; it has an oblong shaped sporangia (~1.5  $\mu$ m in length) with smooth surface, emerging directly from vegetative mycelium, arranged singly or in clusters. Globose bodies (~2.0  $\mu$ m in

diameter) were also observed. It is a mesophilic strain, growing well at 28 °C and up to 45 °C on ISP2 agar.

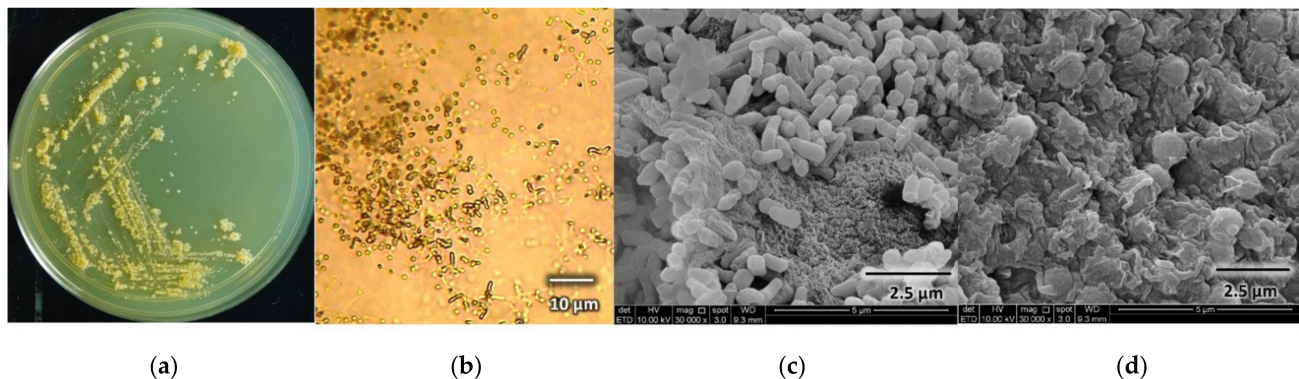


**Figure 4.** *Dactylosporangium* sp. AC04546 morphology: (a) surface morphology on Yeast Malt Extract (ISP2) agar; (b) spore-forming structures viewed using light microscope at 750× magnification on Soil Extract agar (SEA); (c) oblong-shaped sporangia viewed using scanning electron microscope (SEM Quanta FEG 650); (d) globose bodies viewed using scanning electron microscope (SEM Quanta FEG 650).

### 3.5.2. *Dactylosporangium* sp. AC04546 Taxonomic Delineation

The complete 16S rRNA gene sequence for *Dactylosporangium* sp. AC04546 (1361 bp) was used for online BLASTN analysis against the 16S ribosomal RNA sequences (Bacteria and Archaea). *Dactylosporangium* sp. AC04546 had a 99.85% identity to *Dactylosporangium sucinum* strain RY35-23 (NR\_145935.1) and genome-based phylogeny also shows that they are closely related (Figure 5) (TYGS, <https://tygs.dsmz.de>, accessed on 25 June 2021). Bacterial species are defined as including strains that present 95.00–96.00% of average nucleotide identity (ANI) and 70.00% of digital DDH (dDDH) [61]. Due to the low dDDH value of 44.40%, Average Amino Acid identity (AAI) was carried out [73]. Kostas lab server (<http://enve-omics.ce.gatech.edu/g-matrix/>, accessed on 27 June 2021) was used for this purpose. Amino acid sequences for *Dactylosporangium sucinum* JCM 19831 was obtained from NCBI Genome Assembly data (<https://www.ncbi.nlm.nih.gov/assembly>, accessed on 5 July 2021). AAI comparison resulted in a similarity of 89.64%. Accordingly, strains from the same microbial species share >95.00% Average Amino Acid Identity (AAI) [74].

ANI estimate of 91.63%, AAI of 89.64% and dDDH of 44.40% suggests that *Dactylosporangium* sp. AC04546 is a separate species from *Dactylosporangium sucinum*.

### 3.5.3. *Dactylosporangium* sp. AC04546 Genomic Attributes

- Genomic & Protein Features

The draft genome for *Dactylosporangium* sp. AC04546 (JAHYSG000000000) has a size of approximately 13 kb (13,028,014) with a DNA G+C content of 72.1 mol%. The draft genome has a capacity for 12,556 protein encoding genes as well as rRNAs [5S (1), 16S (4), 23S (3)] and 88 tRNAs. *Dactylosporangium* sp. AC04546 draft genome consists of 16% subsystem coverage which contributes to a total of 334 subsystems out of 12,556 CDS predicted by the RAST server (Supplementary Figure S5 Predicted proteins were further analyzed into different functional classes using Cluster of Orthologous Groups (COGs) (Figure A2, Appendix B). Out of 7006 proteins, 4995 were mapped to unique COGs which were further classified into metabolism (33.93%), cellular processes and signaling (32.82%), information storage and processing (17.40%) and poorly characterized (19.86%) functional classes. The remaining 13.39% proteins were assigned to more than one COGs category and were grouped into Multiple COG. A total of 11 confirmed CRISPR loci, indicates the high ability of *Dactylosporangium* sp. AC04546 naturally occurring genome editing system which serves as genome editing sites (Table A7, Appendix B).

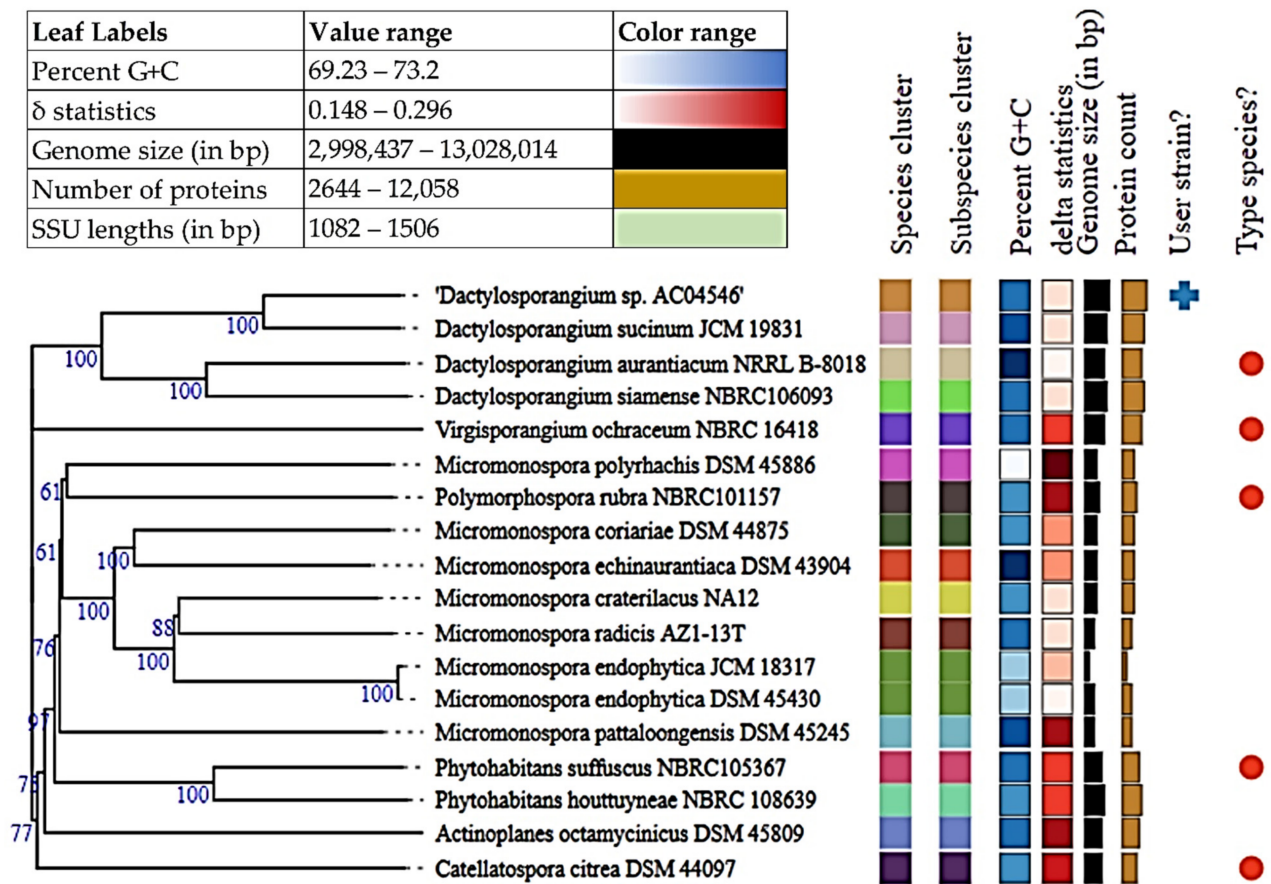


**Figure 5.** Tree inferred with FastME 2.1.6.1 (Lefort et al., 2015) from GBDP distances calculated from genome sequences. The branch lengths are scaled in terms of GBDP distance formula  $d_5$ . The numbers above branches are GBDP pseudo-bootstrap support values > 60% from 100 replications, with an average branch support of 81.9%. The tree was rooted at the midpoint [62].

- Specialty Gene:

Antibiotic-resistant genes, 2 genes (strict criteria) with functions in antibiotic resistance towards aminoglycoside (ARO:3002644) and glycopeptide antibiotic (ARO:3005036) were detected (Table A8). Two drug targets were detected using PATRIC 539 server and verified using DRUGBANK, 1 putative gene encoding GTP binding (Pfam: 540 Tubulin (Pfam: PF00091) and FtsZ\_C (Pfam: PF12327) and 1 putative gene encoding re-541 combinase A, Rec A (Pfam: PF00154) (Table A9).

- Secondary metabolite clusters:

AntiSMASH software predicted 19 secondary metabolite biosynthetic gene clusters (BGCs) (Table A10). Two BGCs showed more than 50% similarity to arenimycin (68%) and alkyl-O-dihydrogeranyl-methoxyhydroquinones (57%), respectively, 10 BGCs below 50%, and 7 BGCs with no similarity.

- Urea Metabolism:

Based on the draft genome of *Dactylosporangium* sp. AC04546, it is predicted to be able to utilize urea as the sole nitrogen source during N-limiting conditions. Presence of putative genes for urea transporters (*urtA*, *urtB*, *urtC*, *urtD*, *urtE*) and urease operon (*ureA*, *ureB*, *ureC*, *ureD*, *ureE*, *ureF*, *ureG*) were identified [75] (Table A11). The potential of using *Dactylosporangium* sp. AC04546 strain or enzyme for bioremediation expands beyond rubber biodegradation.

- Polyhydroxybutyrate Metabolism

A total of 88 putative genes involved in polyhydroxybutyrate metabolism were found. Six scenarios were predicted by The SEED Viewer but were incomplete (Figure A3). Poly-3-hydroxybutyrate (PHB) is a biological polyester present in bacteria and eukaryotic cells stored for carbon and energy storage during stress, and is extensively studied for production of biodegradable plastics [76].

### 3.5.4. Identification of Latex Clearing Protein (Lcp) Homolog for *Dactylosporangium* sp. AC04546

NCBI Conserved Domain Database (CDD) search, shows that *Dactylosporangium* sp. AC04546 lcp-homologs (*lcp1*, *lcp2* and *lcp3* gene) belong to the DUF2236 domain-containing protein (accession pfam 09995). All the lcp-homologs contains the 13-residue long conserved region.

The operon structure (*lcp-oxiAB*) of *Dactylosporangium* sp. AC04546 is similar to previously reported strains containing 3-lcp homologs; *Streptomyces* sp. CFMR-7 [77] and *Actinoplanes* sp. strain OR16 [78], whereby 2-lcp homologs are located adjacent to each other, followed by *oxiAB* genes, with 1-lcp homolog located far apart (Figure 6). The *lcp2* and *lcp3* gene for *Dactylosporangium* sp. AC04546 were located adjacent to each other on contig 82, while *lcp1* gene was located on contig 1 (Figure 6). Amino acid sequences of Lcp2 and Lcp3 are 60.8% similar. Amino acid sequences for Lcp1 and Lcp2 have a similarity of 48.3% while Lcp1 and Lcp3 have a 45.3% similarity.

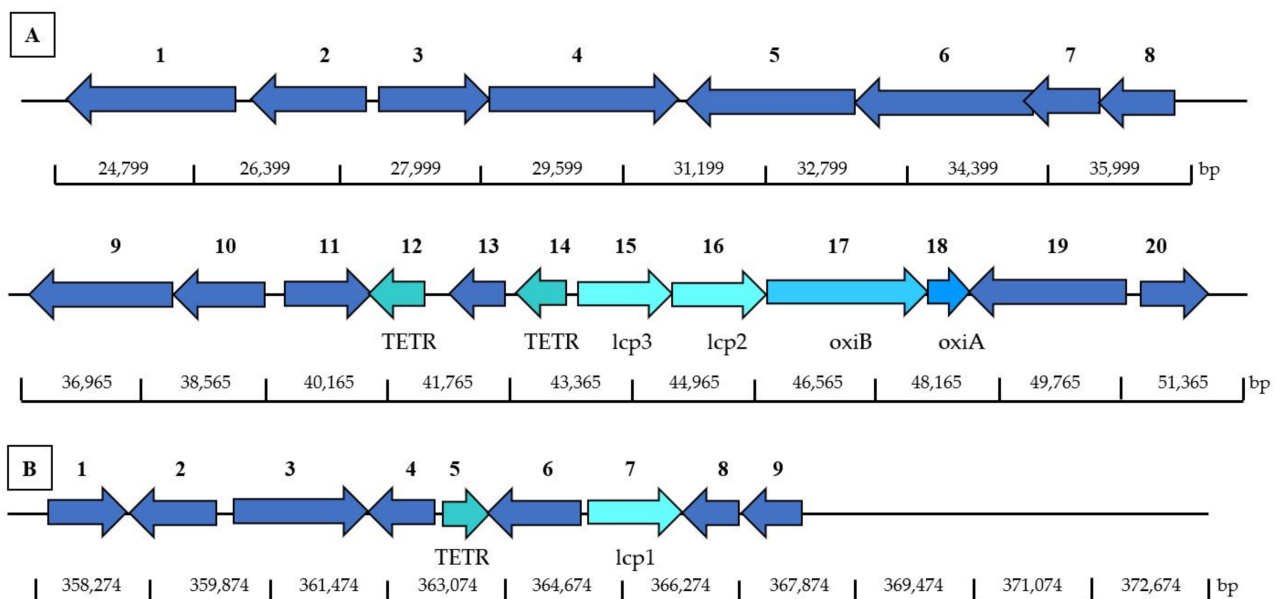


**Figure 6.** Location of *lcp1*, *lcp2* and *lcp3*, and adjacent genes in *Dactylosporangium* sp. AC04546 located on chromosome: (A) Contig 82: 1, Long chain fatty acid CoA ligase (EC 6.2.1.3); 2, Transcriptional regulator, AcrR; 3, Acetyl-CoA Acetyl-transferase (EC 2.3.1.9); 4, Enoyl-CoA Hydratase [isoleucine degradation] (EC 4.2.1.17)/3-Hydroxyl-CoA dehydrogenase (EC 1.1.1.35)/3-Hydroxyl-CoA butyryl CoA epimerase (EC 5.1.2.3); 5, Long chain fatty acid CoA ligase (EC 6.2.1.3); 6, Oxidoreductase, GMC family; 7, ABC transporter; 8, branch chain amino acid transport ATP-binding protein LivG; 9, High affinity branched chain amino acid transport system permease protein LivH (TC 3.A.1.4.1); 10, ABC transporter substrate binding protein; 11, Acyl-CoA dehydrogenase; 12, Transcriptional regulator, TETR family; 13, oxidoreductase, short chain dehydrogenase/reductase family; 14, Transcriptional regulator, TETR family; 15, latex clearing protein gene 3 (*lcp3*); 16, latex clearing protein gene 2 (*lcp2*); 17, Isoquinoline 1-oxidoreductase beta subunit (*oxiB*); 18, Isoquinoline 1-oxidoreductase alpha subunit (*oxiA*); 19, GGDEF domain containing protein; 20, RNA polymerase sigma-70 factor. (B) Contig 1: 1, S8 family serine peptidase; 2, hypothetical protein; 3, two component system sensor histidine kinase; 4, NmrA family protein; 5, Transcriptional regulator, TETR family; 6, Transcriptional regulator, AcrR family; 7, latex clearing protein gene 1 (*lcp1*); 8, HTH-type transcriptional activator TipA; 9, two component system sensor histidine kinase.

The *lcp1* gene (MW659700) is located on contig 1 from 364,865 to 366,085 bp. CDS translation results in 407 amino acids, encoding a protein with a theoretical mass of 44.2 kDa and 9.00 pI. Twin arginine translocation (TAT) signal peptide cleavage site was predicted to be between 40 and 41 bp (ALA-AP). Putative ribosomal site (RBS) was detected at 6 bp upstream from the putative start codon. The *lcp1* gene (1221 bp) showed 80.70% blast homology to latex clearing protein of *Amycolatopsis* sp. YIM 10 (A0A5P9PKU1\_9PSEU). Lcp1 amino acid sequence a 40.70% similarity to characterized Lcp of *Gordonia polyisoprenivorans* VH2.

The *lcp2* gene (MW659701) is located on contig 82 from 43,562 to 44,770 bp. CDS translation results in 403 amino acids, encoding a protein with a theoretical mass of 43.8 kDa and 6.33 pI. Twin arginine translocation (TAT) signal peptide cleavage site was predicted to be between 40 and 41 bp (AGA-GA). Putative ribosomal site (RBS) was detected at 9 bp upstream from the putative start codon ATG. The *lcp2* gene (1200 bp) showed 87.60 % blast homology to latex clearing protein of *Nonomuraea* sp. ATCC 55076 (A0A1U9ZY53\_9ACTN). Lcp1 amino acid sequence had a 65.33% similarity to Lcp of *Gordonia polyisoprenivorans* VH2 characterized.

The *lcp3* gene (MW659702) is located on contig 82 from 44,862 to 46,061 bp. CDS translation results in 400 amino acids, encoding a protein with a theoretical mass of 43.9 kDa and 5.93 pI. Twin arginine translocation (TAT) signal peptide cleavage site was predicted between 40 and 41 bp (AGA-GA). Putative ribosomal site (RBS) was detected at 9 bp upstream from the putative start codon ATG. The *lcp3* gene (1224 bp) showed 84.00% blast homology to latex clearing protein of *Actinophytocola xinjiangensis* (A0A7Z0WP15\_9PSEU). Lcp1 amino acid sequence had a 50.63% similarity to characterized Lcp of *Gordonia polyisoprenivorans* VH2 (ABV68923.1).

### 3.5.5. Predicted Genes Involved in Rubber Degradation for *Dactylosporangium* sp. AC04546

Putative genes that may participate in the rubber degradation in *Dactylosporangium* sp. AC04546 were identified in its draft genome (Table A12). Five putative TER-family gene were identified, 2 genes located 119 bp and 2218 bp downstream of the *lcp2*, *lcp3*. One gene belonging to the TETR-family, located 1431 bp downstream *lcp1* gene, could be involved in the Lcp transcription (Figure 6). Lcp are secreted outside the bacterial cell via twin-arginine translocation (TAT) pathway. Four putative gene-coding TAT proteins (*TatA*, *TatB*, *TatC*) were identified. The *oxiAB* gene, located downstream of the *lcp3* and *lcp2* gene, is an oxidoreductase that converts the oligo-isoprenoid terminal aldehyde group to a carboxylic acid group. Oligo-isoprenoids are then transported into the bacterial cell. No specific MCE-family genes were detected. The resulting isoprenoid acids enter the  $\beta$ -oxidation cycle and are converted into acyl-CoA thioester by an acyl-CoA synthase (2 candidate gene). Acyl-CoA thioester are further catabolized by an acyl-CoA dehydrogenase (EC 1.3.8.1 & EC 1.3.8.8) (6 candidate genes). Polyunsaturated fatty acids degradation occurs when 2,4-dienoyl-CoA reductase (EC 1.3.1.34) (1 candidate genes) catalyzes double bonds at the even-numbered position, followed by isomerization by enoyl-CoA hydratases (EC 4.2.1.17) (14 candidate genes). Fourteen homologous genes for 3-hydroxyacyl-CoA dehydrogenases (EC 1.1.1.35) were identified, possibly involved in the following hydration step, responsible for the conversion of the hydroxyl derivatives into the keto. The last step of the first-oxidation cycle is predicted to be catalyzed by the thiolase/3-ketoacyl-CoA thiolase (EC 2.3.1.16) (15 candidate genes).

Mutants with a disruption of the  $\alpha$ -methylacyl-CoA racemase (*Mcr*) gene lost the ability to metabolize poly-(*cis*-1,4-isoprene) and related methyl-branched isoprenoid compounds (Arenskötter et al., 2008). Three *Mcr* genes (EC 5.1.99.4) were also identified in the genome of *Dactylosporangium* sp. AC04546.

The presence of these genes in the genome of *Dactylosporangium* sp. AC04546 suggests that this genome may share the same rubber degradation pathway as predicted previously.

### 3.6. Utilization of Rubber Materials by *Microtetraspora* sp. AC03309 and *Dactylosporangium* sp. AC04546

When cultivated in an ISP2 broth at 28 °C, 180 rpm, *Microtetraspora* sp. AC03309 was actively growing by Day 7 while *Dactylosporangium* sp. AC04546 by Day 10. Actively growing culture was used to inoculate Mineral Salts Medium (MSM) containing rubber as the sole carbon source. Rubber utilization studies were conducted separately for both strains.

After 30 days of incubation, SEM images of rubber materials showed that the strains were able to grow and utilize fresh latex, latex glove, or tyres as the sole carbon and energy source. The biodegradation of the rubber polymer begins with microbial attachment on the surface, which has thread-like appearances (yellow arrow) in comparison to non-inoculated samples [Figure 7]. Once attached, the microorganism releases degrading enzymes through its mycelia, initiating the first step of rubber degradation. This can be seen through the presence of rough, cracked, and holes (white arrow) on the rubber materials [Figure 7b,c].

### 3.7. ATR-FTIR Analysis of Degraded Rubber Materials

ATR-FTIR spectroscopy is a useful tool to determine the formation or disappearance of functional groups of materials that indicate degradation of the original material. The infrared spectroscopy (IR) can be divided into 4 categories: (i) single bond area ( $4000\text{ cm}^{-1}$ – $2500\text{ cm}^{-1}$ ), (ii) triple bond region ( $2500\text{ cm}^{-1}$ – $2000\text{ cm}^{-1}$ ), (iii) double bond region ( $2000\text{ cm}^{-1}$ – $1500\text{ cm}^{-1}$ ) and (iv) fingerprint region ( $1500\text{ cm}^{-1}$ – $600\text{ cm}^{-1}$ ) [79]. During rubber utilization, Lcp catalyzes the oxidative C-C cleavage of poly(*cis*-1,4-isoprene) in natural rubber as well as in synthetic rubber by the addition of oxygen ( $\text{O}_2$ ) to the double bonds, leading to a mixture of oligonucleotide-isoprenoids with terminal keto and aldehyde groups (endo-type cleavage) [9,11,80].

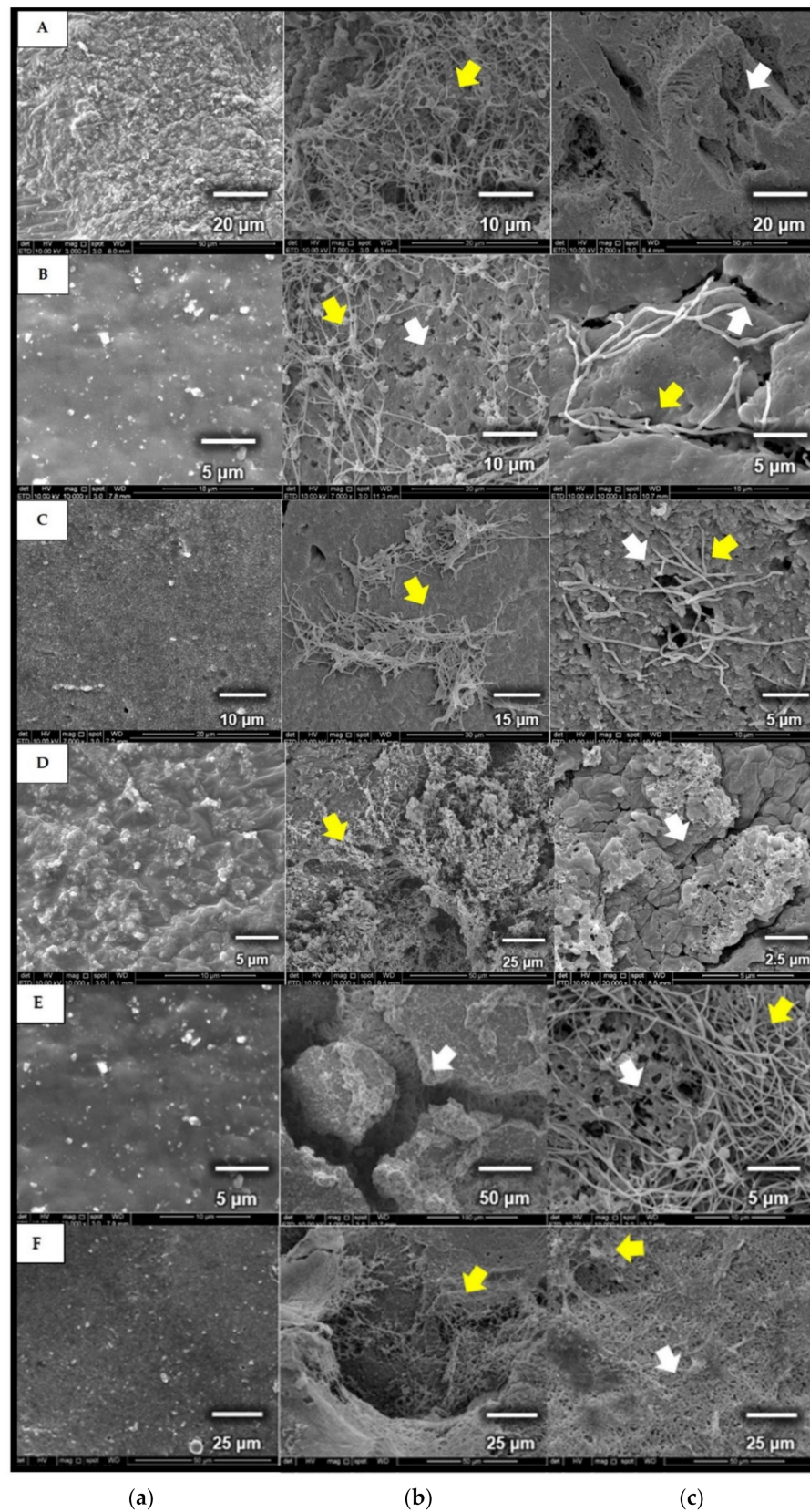
#### 3.7.1. Fresh Latex ATR-FTIR Profile

Figure 8 shows the ATR-FTIR profile for fresh latex (A) control, no microbial culture added, (B) cultivated with *Dactylosporangium* sp. AC04546, and (C) cultivated with *Microtetraspora* sp. AC03309.

Characteristic bands of the polyisoprene chain at  $2962\text{ cm}^{-1}$ ,  $2928\text{ cm}^{-1}$  and  $2855\text{ cm}^{-1}$  were present [81]. Decreased intensity of this spectrum for *Dactylosporangium* sp. AC04546 and *Microtetraspora* sp. AC03309 indicates the degradation of fresh latex samples. Degradation of fresh latex should result in the appearance of hydroxyl, carbonyl (aldehyde, ketone, and/or carboxylic acid) and ester groups [81]. A range of between  $1750\text{ cm}^{-1}$  and  $1700\text{ cm}^{-1}$  describes simple carbonyl compounds (ketones, aldehydes, esters, or carboxyl). Peak below  $1700\text{ cm}^{-1}$  corresponds to carbonyl with amides or carboxylates functional group, while intensity at between  $1650\text{ cm}^{-1}$  and  $1600\text{ cm}^{-1}$  is due to the presence of double bonds. Strong peak profile at  $1200\text{ cm}^{-1}$ – $1000\text{ cm}^{-1}$  for *Dactylosporangium* sp. AC04546 is caused by C-O-C stretching vibration in esters. Similar changes of profile was also reported in natural rubber after 1 year aging at temperate temperature compared to control [82].

#### 3.7.2. Latex Glove ATR-FTIR Profile

Figure 9 shows the ATR-FTIR profile for latex gloves in MSM with (A) control, no microbial culture added, (B) *Dactylosporangium* sp. AC04546, and (C) *Microtetraspora* sp. AC03309. Characteristic bands of the polyisoprene chain at  $2962\text{ cm}^{-1}$ ,  $2928\text{ cm}^{-1}$  and  $2855\text{ cm}^{-1}$  [81] were also present in the latex glove profiles. A broad absorption band in the range of  $3650$  and  $3250\text{ cm}^{-1}$  for *Dactylosporangium* sp. AC04546 and *Microtetraspora* sp. AC03309, is caused by O-H stretching vibrations in the carboxylic groups, as a result of rubber degradation by oxidation. At  $1750\text{ cm}^{-1}$ – $1725\text{ cm}^{-1}$  a distinct peak for ester was detected in the profile for *Dactylosporangium* sp. AC04546. While a distinct peak at  $1680$ – $1630\text{ cm}^{-1}$  for amide appeared in the IR for *Microtetraspora* sp. AC03309, obvious change in the peak profile at  $1200$ – $1000\text{ cm}^{-1}$  was caused by C-O-C stretching vibration in esters.



**Figure 7.** Micrographs of (a) control, rubber samples without microbial cultivation (A & D: fresh latex pieces; B & E: latex glove pieces; C & F: tyre granules); (b,c) rubber samples used as carbon source for cultivating *Microtetraspora* sp. AC03309 (A,B,C) and *Dactylosporangium* sp. AC04546 (D,E,F), incubated for 30 days, 28 °C at 180 rpm.

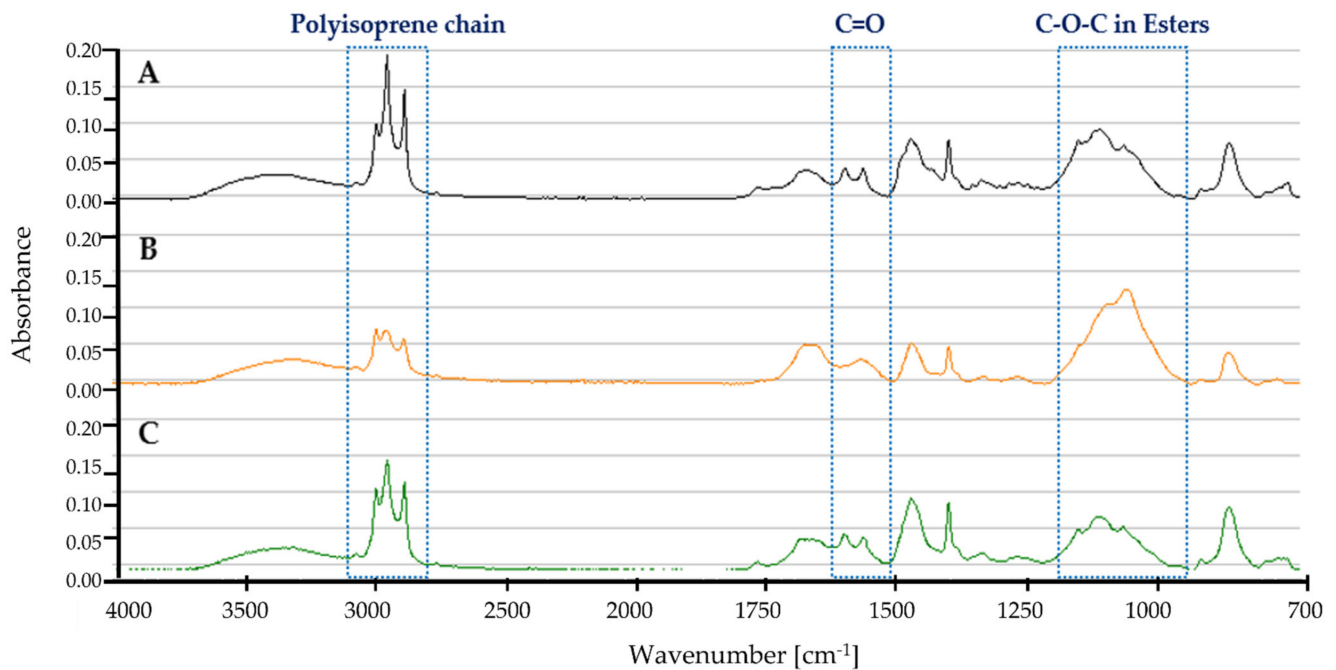


**Figure 8.** ATR-FTIR profile for fresh latex pieces as carbon source in MSM broth for 30 days, 28 °C, 180 rpm (A) Control (B) *Dactylosporangium* sp. AC04546 (C) *Microtetraspora* sp. AC03309.

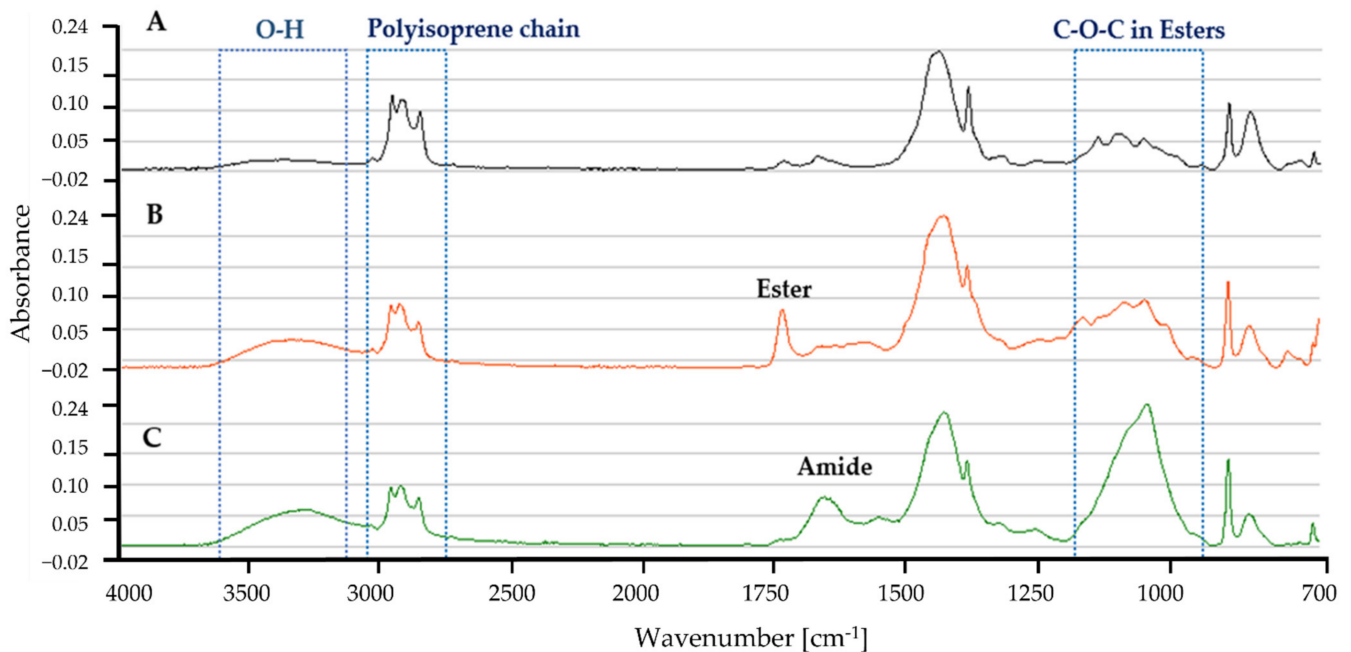


**Figure 9.** ATR-FTIR profile for latex glove strips as carbon source in MSM broth for 30 days, 28 °C, 180 rpm (A) Control (B) *Dactylosporangium* sp. AC04546 (C) *Microtetraspora* sp. AC03309.

### 3.7.3. Tyre ATR-FTIR Profile

Based on the IR spectra, tyre samples incubated with *Dactylosporangium* sp. AC04546 showed differences at  $3000\text{ cm}^{-1}$  and  $\sim 1000\text{ cm}^{-1}$  (Figure 10). The broadening of peaks at  $\sim 3000\text{ cm}^{-1}$  is caused by C-H, O-H and N-H stretching, while peak intensity at  $\sim 1000\text{ cm}^{-1}$  is due to stretching vibrations of the C-C and/out of plane deformation of C=C-H [83].

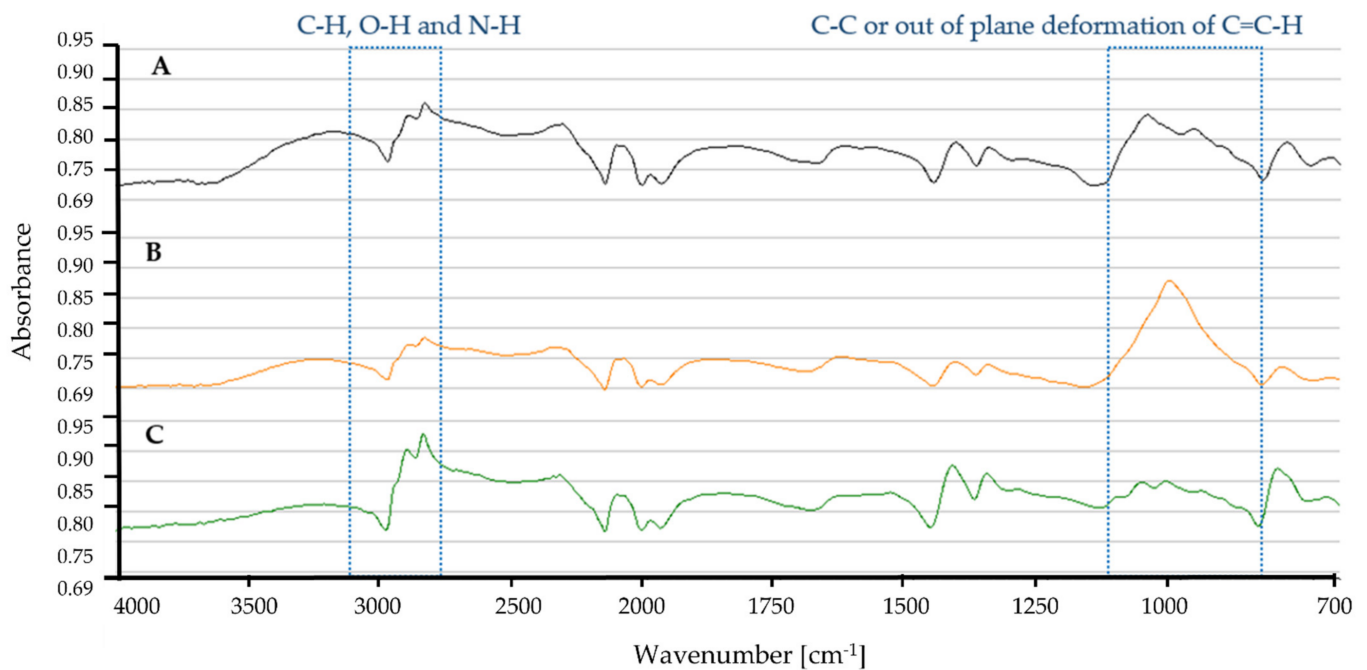


**Figure 10.** ATR-FTIR profile for tyre granules as carbon source in MSM broth for 30 days, 28 °C, 180 rpm (A) Control (B) *Dactylosporangium* sp. AC04546 (C) *Microtetradora* sp. AC03309.

#### 4. Discussion

We were able to quickly screen a portion of SBC Actinobacterial Culture Collection by modifying the screening method using natural rubber (NR) latex agar in 6-well plates instead of latex agar overlay technique as described by Braaz et al., (2004) [28]. We also prolonged the incubation period from 1 week to 4 weeks as some Actinobacteria strains (rare group) are known to be slow growers. Using 6-well plates, we prepared NR latex agar (without overlay) in smaller volume while utilizing minimal space. The separation of media by wells also avoids cross contamination, especially by sporulating strains. A similar method using NR latex agar in 24-well plates was not successful in detecting the formation of clear zones. Using MSM broth added with NR latex in test tubes, 6-well plate and 24-well plate did not show changes in the turbidity of the medium.

Back in 1997, a publication indicated that *Microtetradora* sp. strain 3880-19B isolated from a soil sample collected in Malaysia, and *Dactylosporangium thailandense* DSM 43158 isolated from Thailand produced clearing zone on NR latex overlay agar [21]. However, no further studies on these strains have been reported. No molecular information or strain deposition was found for *Microtetradora* sp. strain 3880-19B. When we compared the genome of *Microtetradora* sp. AC03309 and *Microtetradora glauca* strain NBRC 14761 using The SEED Viewer server, *Microtetradora glauca* strain NBRC 14761 did not contain genes of Lcp-homolog, isoquinoline 1-oxidoreductase beta subunit (oxiB), isoquinoline 1-oxidoreductase alpha subunit (oxiA) and MCE-family protein. The genome search of *Microtetradora glauca* using the GenBank database also confirms this. Only 1 genome for *Microtetradora glauca* has been deposited to the NCBI Genome database. Although in silico taxonomic delineation classifies *Microtetradora* sp. AC03309 as a novel subspecies under *Microtetradora glauca*, based on the rubber-degrading ability and related rubber degradation gene content, we propose *Microtetradora* sp. AC03309 to be considered as a novel species. In this study, we have successfully identified 7 *Microtetradora* strains containing Lcp-homolog. It would be interesting also to look at the interspecies variation.

Comparison between 16S rDNA sequence of *Dactylosporangium* sp. AC04546 and *Dactylosporangium thailandense* DSM 43158 showed a similarity of 98.00%, which is below the recommended threshold of >98.65% 16S rRNA gene sequence similarity for differentiating two species [60]. Therefore, we believe both strains to be distinct. We then compared

the genome of *Dactylosporangium* sp. AC04546 to *Dactylosporangium sucinum* JCM 19831. Interestingly, we found 3-Lcp homologs, putative *oxiB* and putative *oxiA* genes within the *Dactylosporangium sucinum* JCM 19831 genome. The *lcp3* gene and the *lcp2* gene were located on contig 30 together with *oxiAB*, while *lcp1* was located on contig 19 of *Dactylosporangium sucinum* JCM 19831. When we compared the Lcp-homologs amino acid sequence, Lcp1 of both sequences had a 95.07% similarity, Lcp2 had a 93.03% similarity and Lcp3 had a 97.24% similarity. Four MCE-family proteins were detected in the draft genome of *Dactylosporangium sucinum* JCM 19831 (genome size 12,103,263 bp) and was compared to the genome of *Dactylosporangium* sp. AC04546 (genome size 13,028,014 bp). No blast homology was detected. Therefore, further analysis of the *Dactylosporangium* sp. AC04546 membrane transporter proteins involved in the rubber degradation pathway are needed. Low ANI and dDDH values for *Dactylosporangium* sp. AC04546 to *Dactylosporangium sucinum* JCM 19831 suggest that they have distinct genomic differences as a separate species, while the full length Lcp amino acid comparison did not match 100.00%.

Almost all rubber-degrading Actinobacteria, including *Streptomyces*, *Nocardia*, and *Rhodococcus* species have a single Lcp homolog [78]. We predict that Actinobacterial strains adapt by incorporating lcp genes into their chromosome through their plasmid (e.g., *Gordonia polyisoprenivorans* VH2, 1 lcp gene in plasmid and in 1 lcp gene in its chromosome). Actinobacteria have been known to adapt quickly through incorporation of genes (horizontal gene transfer, HGT). The question is whether the incorporation of Lcp-homologs impact the ability of the strain to utilize and degrade different rubber products? Previous reports indicate that different Lcp produce a variety of rubber degraded products (molecular weight, number of isoprene units, functional groups, etc) [65]. This could most likely be due to the different or synergistic mechanism of Lcp, which is yet to be explored. Lcp genes from *Microtetraspora* sp. AC03309 and *Dactylosporangium* sp. AC04546 also did not cluster with other biochemically characterized Lcp (Supplementary Figure S6).

Dissimilar to other rubber products, tyres are made from vulcanized rubber and ~30% carbon black for reinforcement, rendering them more resistant to degradation. Vulcanization of rubber material through sulfur interlinkages of the poly(*cis*-1,4-isoprene) chains results in reduced water absorption and gas permeability of the material [65]. Based on the rubber utilization studies, we observed that both strains were able to colonize and utilize various rubber products differently. An obvious observation was the ability of *Dactylosporangium* sp. AC04546 to colonize the tyre samples effectively through excretion of rubber-degrading enzymes (appearance of holes on the tyre surface compared to control and samples incubated with *Microtetraspora* sp. AC03309). This is supported by the changes detected in the ATR-FTIR profile. Since tyres are the second largest contributor to microplastic pollution in the ocean [84], it would be interesting to study the potential of *Dactylosporangium* sp. AC04546 in degrading tyre wastes.

Most of the clear zone producing strains (61%) were isolated from soil samples collected from Kiding Village Forest area. The Kiding village settlement was founded in the 1840s and is located 1300 m above sea level; it is only accessible by a 3-h hike. While all the other NR latex degrading strains were isolated from secondary forest soil samples, the isolation sites for all the strains have no obvious rubber wastes or rubber materials present, so there does not appear to be an apparent evolutionary pressure for the appearance of lcp genes. Nonetheless, these strains do degrade rubber, and it is possible that this function may have been triggered by the presence of rubber particles dispersed in the environment. Recent studies have shown that rubber particles from sources such as tyres are widely dispersed. Sieber et al., (2020), estimated that 218 ktons of rubber particles from tyres are mainly deposited on road-side soils (74%), surface water (22%) and in soils (4%) [85]. Alternatively, the presence of latex producing plants in the vicinity may have contributed to the development of Lcp in these strains. Further studies would be required to confirm the reasons for this. But this observation highlights the importance of surveying microorganisms from diverse ecosystems (e.g., marine, or freshwater bodies) for their genomic background and functional ability related to biodegradation of rubber or other pollutants.

## 5. Conclusions

Miniaturized random screening using Sarawak's Actinobacterial Culture Collection led to the successful identification of 18 natural rubber latex degrading Actinobacteria isolated from environmental soil samples. Two rare Actinobacteria strains with uncharacterized lcp genes, *Microtetraspora* sp. AC03309 and *Dactylosporangium* sp. AC04546 were explored. *Microtetraspora* sp. AC03309 a proposed novel species has 2 Lcp homologs on its chromosome, while *Dactylosporangium* sp. AC04546 is a proposed novel species that has 3 Lcp homologs on its chromosome. The identification of genes predicted to be involved in the rubber-degradation pathway was established for both strains and corresponds to the genes identified in other rubber-degrading Actinobacteria. The presence of other assimilation genes such as sulfur in *Microtetraspora* sp. AC03309, and urea and polyhydroxybutyrate in *Dactylosporangium* sp. AC04546 provides them with added advantages as biodegraders. Both strains were also able to colonize and utilize rubber-based materials within 30 days of incubation. Interestingly, *Dactylosporangium* sp. AC04546 grew well in the presence of tyre samples as the sole carbon and energy source, showing visible changes on the tyre surface seen in SEM images and changes in the ATR-FTIR spectra within 30 days of incubation. Further studies on the ability of this strain (or a combination of strains) to effectively degrade tyre products and detailed analysis of the degraded rubber products would be of interest for future research.

**Supplementary Materials:** The following are available online at <https://www.mdpi.com/article/10.3390/polym13203524/s1>, Figure S1: Research approach flow chart; Figure S2: Clear zone forming strains 16S rRNA evolutionary relationships of taxa together with top 1 blast homology in GenBank database; Figure S3: Latex clearing protein (Lcp) amino acid sequence alignment of the 18 clear zone strains to determine the 13-residue long highly conserved region; Figure S4: Subsystem distribution in *Microtetraspora* sp. AC03309; Figure S5: Subsystem distribution in *Dactylosporangium* sp. AC04546; Figure S6: Phylogenetic tree of characterized Lcps and Lcps from *Microtetraspora* sp. AC03309 and *Dactylosporangium* sp. AC04546.

**Author Contributions:** A.A.B.: Data Curation, Writing—Original Draft, Investigation, Formal Analysis, Visualization, Funding Acquisition, J.N.: Resources, Writing—Review and Editing, T.C.Y.: Project Administration, Funding Acquisition, K.S.: Supervision Project, Conceptualization, Writing—Review and Editing. All authors have read and agreed to the published version of the manuscript.

**Funding:** This work was supported by the Government of Sarawak under USM grant number 304.PBIOLOGI.6501009.J136.

**Data Availability Statement:** Contigs used in this study were deposited into the National Centre for Biotechnology Information (NCBI) database; *Microtetraspora* sp. AC03309 under the BioProject ID: PRJNA668755, with BioSample Accessions SUB8307686 and *Dactylosporangium* sp. ACO4546 under the BioProject ID: PRJNA749440, with BioSample Accessions SUB10069292. All the other data supporting the findings of this study are available in this published article and its supplementary information files.

**Acknowledgments:** We would like to acknowledge the Sarawak Government for providing research funds to conduct this study. Also acknowledging the Sarawak Biodiversity Centre (SBC) staff especially those working in the Microbiology Group and the Molecular Group. We would also like to express our appreciation to the Ecobiomaterial Lab members of USM for their support. Special thanks to Gincy P. Thottathil (Ecobiomaterial Lab, USM) for her guidance in primer designs and Mohd. Farith Bin Kota (Microbiology Lab, SBC) for providing SEM images for *Microtetraspora* sp. AC03309.

**Conflicts of Interest:** The authors declare no conflict of interest.

## Appendix A



**Figure A1.** Cluster of Orthologous (COGs) for *Microtetraspora* sp. AC03309 analyzed using egg-NOG mapper v.2 [42]. CELLULAR PROCESSES AND SIGNALING [D] Cell cycle control, cell division, chromosome partitioning, [M] Cell wall/membrane/envelope biogenesis, [N] Cell motility; [O] Post-translational modification, protein turnover, and chaperones, [T] Signal transduction mechanisms, [U] Intracellular trafficking, secretion, and vesicular transport, [V] Defense mechanisms [W] Extracellular structures, [Y] Nuclear structure, [Z] Cytoskeleton; INFORMATION STORAGE AND PROCESSING [A] RNA processing and modification, [B] Chromatin structure and dynamics, [J] Translation, ribosomal structure and biogenesis, [K] Transcription, [L] Replication, recombination and repair; METABOLISM [C] Energy production and conversion, [E] Amino acid transport and metabolism, [F] Nucleotide transport and metabolism, [G] Carbohydrate transport and metabolism, [H] Coenzyme transport and metabolism, [I] Lipid transport and metabolism, [P] Inorganic ion transport and metabolism, [Q] Secondary metabolites biosynthesis, transport, and catabolism; POORLY CHARACTERIZED [R] General function prediction only, [S] Function unknown.

**Table A1.** *Microtetraspora* sp. AC03309 CRISPR array detected from CRISPRFinder server.

|   | Contig       | Start (bp) | Stop (bp) |
|---|--------------|------------|-----------|
| 1 | contig000014 | 94,175     | 94,462    |
| 2 | contig000145 | 766        | 977       |

**Table A2.** *Microtetraspora* sp. AC03309 antibiotic resistant gene identified using CARD database.

|   | Contig        | Start (bp) | Stop (bp) | Classification                     | Identity (%) |
|---|---------------|------------|-----------|------------------------------------|--------------|
| 1 | contig000052  | 61,507     | 62,700    | elfamycin (ARO: 3003361)           | 77           |
| 2 | contig 000084 | 35,081     | 36,280    | rapamycin antibiotic (ARO:3002883) | 93           |

**Table A3.** *Microtetraspora* sp. AC03309 drug target gene identified using PATRIC server and DrugBank server.

|   | Contig       | Product                                           | Start (bp) | Stop (bp) | Length (bp) | Query Coverage | Identity (%) |
|---|--------------|---------------------------------------------------|------------|-----------|-------------|----------------|--------------|
| 1 | Contig000007 | RecA protein                                      | 27,312     | 25,081    | 1104        | 88             | 85           |
| 2 | Contig000641 | Serine/threonine-protein kina, pknB (EC 2.7.11.1) | 35         | 322       | 288         | 90             | 88           |
| 3 | Contig000054 | Cell division protein, ftsZ                       | 15,100     | 13,667    | 1434        | 95             | 92           |

**Table A4.** *Microtetraspora* sp. AC03309 putative genes involved in sulfur assimilation annotated using RAST server.

|                                                         | Roles                                                                             | ORF |
|---------------------------------------------------------|-----------------------------------------------------------------------------------|-----|
| <b>Inorganic sulfur: Sulfate/thiosulfate metabolism</b> |                                                                                   |     |
| 1                                                       | 3'(2'),5'-bisphosphate nucleotidase (EC 3.1.3.7)                                  | 1   |
| 2                                                       | Adenylylsulfate kinase (EC 2.7.1.25)                                              | 2   |
| 3                                                       | Adenylyl-sulfate reductase [thioredoxin] (EC 1.8.4.10)                            | 3   |
| 4                                                       | Ferredoxin                                                                        | 12  |
| 5                                                       | Ferredoxin-like protein involved in electron transfer                             | 1   |
| 6                                                       | Ferredoxin-NADP(+) reductase, actinobacterial (eukaryote-like) type (EC 1.18.1.2) | 1   |
| 7                                                       | Ferredoxin-sulfite reductase, actinobacterial type (EC 1.8.7.1)                   | 1   |
| 8                                                       | Phosphoadenylyl-sulfate reductase [thioredoxin] (EC 1.8.4.8)                      | 1   |
| 9                                                       | Putative sulfate permease                                                         | 1   |
| 10                                                      | Sulfate adenylyltransferase subunit 1 (EC 2.7.7.4)                                | 1   |
| 11                                                      | Sulfate adenylyltransferase subunit 2 (EC 2.7.7.4)                                | 1   |
| 12                                                      | Sulfate adenylyltransferase, dissimilatory-type (EC 2.7.7.4)                      | 1   |
| 13                                                      | Sulfate and thiosulfate binding protein CysP                                      | 1   |
| 14                                                      | Sulfate and thiosulfate import ATP-binding protein CysA (EC 3.6.3.25)             | 2   |
| 15                                                      | Sulfate transport system permease protein CysW                                    | 1   |
| <b>Organic sulfur: Alkanesulfonate assimilation</b>     |                                                                                   |     |
| 1                                                       | ABC-type nitrate/sulfonate/bicarbonate transport system, ATPase component         | 1   |
| 2                                                       | ABC-type nitrate/sulfonate/bicarbonate transport system, permease component       | 2   |
| 3                                                       | ABC-type nitrate/sulfonate/bicarbonate transport systems, periplasmic components  | 1   |
| 4                                                       | Alkanesulfonate monooxygenase (EC 1.14.14.5)                                      | 2   |
| 5                                                       | Alkanesulfonates ABC transporter ATP-binding protein                              | 1   |
| 6                                                       | Alkanesulfonates transport system permease protein                                | 3   |
| 7                                                       | Alkanesulfonates-binding protein                                                  | 1   |
| 8                                                       | Alpha-ketoglutarate-dependent taurine dioxygenase (EC 1.14.11.17)                 | 1   |
| 9                                                       | Arylsulfatase (EC 3.1.6.1)                                                        | 1   |
| 10                                                      | FMN reductase (EC 1.5.1.29)                                                       | 1   |
| 11                                                      | Putative arylsulfatase regulatory protein                                         | 1   |

ORF: Open reading frame.

**Table A5.** *Microtetraspora* sp. AC03309 secondary metabolite biosynthetic gene clusters (BGCs) were predicted using AntiSMASH 6.0.

| Region       | Type                         | From (bp) | To (bp) | Most Similar Known Cluster                                                                                                                                    |                                            | Similarity |
|--------------|------------------------------|-----------|---------|---------------------------------------------------------------------------------------------------------------------------------------------------------------|--------------------------------------------|------------|
| Region 5.1   | other                        | 406       | 41,026  |                                                                                                                                                               |                                            |            |
| Region 7.1   | NRPS                         | 58,409    | 104,012 | tetronasin                                                                                                                                                    | Polyketide                                 | 3%         |
| Region 8.1   | redox-cofactor               | 1         | 16,071  |                                                                                                                                                               |                                            |            |
| Region 8.2   | lanthipeptide-class-iv       | 119,417   | 142,221 |                                                                                                                                                               |                                            |            |
| Region 11.1  | lanthipeptide-class-iv       | 4363      | 27,032  | blasticidin S                                                                                                                                                 | Other                                      | 7%         |
| Region 11.2  | NRPS,T1PKS                   | 87,888    | 145,746 | nostopeptolide A2                                                                                                                                             | Polyketide +<br>NRP:Cyclic<br>depsipeptide | 25%        |
| Region 14.1  | T3PKS                        | 105,469   | 141,262 | alkylresorcinol                                                                                                                                               | Polyketide                                 | 66%        |
| Region 16.1  | RiPP-like                    | 121,803   | 132,618 |                                                                                                                                                               |                                            |            |
| Region 17.1  | terpene                      | 20,289    | 46,240  | hopene                                                                                                                                                        | Terpene                                    | 46%        |
| Region 26.1  | terpene                      | 88,473    | 108,659 | frankiamicin                                                                                                                                                  | Polyketide                                 | 14%        |
| Region 28.1  | NRPS                         | 1         | 28,384  | 5-acetyl-5,10-dihydrophenazine-1-carboxylic acid/5-(2-hydroxyacetyl)-5,10-dihydrophenazine-1-carboxylic acid/endophenazine A1/endophenazine F/endophenazine G | Other:Phenazine                            | 8%         |
| Region 34.1  | betalactone, terpene         | 62,313    | 94,083  | geosmin                                                                                                                                                       | Terpene                                    | 100%       |
| Region 39.1  | lanthipeptide-class-iii      | 66,288    | 83,988  |                                                                                                                                                               |                                            |            |
| Region 44.1  | NRPS                         | 1         | 42,513  | acarviostatin I03/acarviostatin I03/acarviostatin III03/acarviostatin IV03                                                                                    | Saccharide                                 | 11%        |
| Region 44.2  | T1PKS,lanthipeptide-class-iv | 48,145    | 75,803  | labyrinthopeptin A2/labyrinthopeptin A1/labyrinthopeptin A3                                                                                                   | RiPP:Lanthipeptide                         | 40%        |
| Region 45.1  | terpene                      | 24,504    | 45,502  |                                                                                                                                                               |                                            |            |
| Region 49.1  | NRPS                         | 1         | 32,408  | herboxidiene                                                                                                                                                  | Polyketide                                 | 3%         |
| Region 57.1  | thiopeptide,LAP              | 33,174    | 64,696  | muraymycin C1                                                                                                                                                 | NRP +<br>Polyketide                        | 7%         |
| Region 61.1  | siderophore                  | 17,145    | 30,431  |                                                                                                                                                               |                                            |            |
| Region 67.1  | NRPS                         | 1         | 50,370  | triacsins                                                                                                                                                     | Other                                      | 25%        |
| Region 71.1  | siderophore                  | 1         | 8702    | desferrioxamine E                                                                                                                                             | Other                                      | 75%        |
| Region 91.1  | lanthipeptide-class-iv       | 3240      | 26,017  | labyrinthopeptin A2/labyrinthopeptin A1/labyrinthopeptin A3                                                                                                   | RiPP:Lanthipeptide                         | 40%        |
| Region 93.1  | NRPS                         | 1         | 28,814  | catenulisporolides                                                                                                                                            | NRP +<br>Polyketide                        | 5%         |
| Region 135.1 | lanthipeptide-class-iii      | 1         | 11,872  | catenulipeptin                                                                                                                                                | RiPP:Lanthipeptide                         | 60%        |

Region, contig of the draft genome; NRPS, Non-ribosomal peptide synthetase cluster; RiPP, ribosomally synthesized and post-translationally modified peptide product (RiPP) cluster; RRE-containing, RRE-element containing cluster; saccharide, Saccharide cluster (loose strictness, likely from primary metabolism); T1PKS, Type I PKS (Polyketide synthase); T2PKS, Type II PKS; T3PKS, Type III PKS.

**Table A6.** Distribution and loci of  $\beta$ -oxidation related putative genes in the draft genome of *Microtetraspora* sp. AC03309 based on RAST server analysis.

| Transcriptional Regulator, TetR Family on the Same Contig as <i>lcp</i> Gene |              |            |           |             |
|------------------------------------------------------------------------------|--------------|------------|-----------|-------------|
|                                                                              | Contig       | Start (bp) | Stop (bp) | Length (bp) |
| 1                                                                            | contig000003 | 19,522     | 18,260    | 1263        |
| 2                                                                            | contig000003 | 28,599     | 29,279    | 681         |

| <b>Twin-Arginine Translocation Protein, TAT Protein (TatA, TatB, TatC)</b>               |               |                   |                  |                    |
|------------------------------------------------------------------------------------------|---------------|-------------------|------------------|--------------------|
|                                                                                          | <b>Contig</b> | <b>Start (bp)</b> | <b>Stop (bp)</b> | <b>Length (bp)</b> |
| 1                                                                                        | contig000002  | 137,788           | 137,363          | 426                |
| 2                                                                                        | contig000113  | 18,270            | 18,629           | 360                |
| 3                                                                                        | contig000133  | 9169              | 9507             | 339                |
| 4                                                                                        | contig000133  | 9535              | 10,389           | 855                |
| <b>Mammalian Cell Entry, Mce (Mce1D, Mce1D)</b>                                          |               |                   |                  |                    |
|                                                                                          | <b>Contig</b> | <b>Start (bp)</b> | <b>Stop (bp)</b> | <b>Length (bp)</b> |
| 1                                                                                        | contig000186  | 1797              | 1339             | 459                |
| 2                                                                                        | contig000629  | 96                | 284              | 189                |
| <b>Acyl-CoA synthase</b>                                                                 |               |                   |                  |                    |
|                                                                                          | <b>Contig</b> | <b>Start (bp)</b> | <b>Stop (bp)</b> | <b>Length (bp)</b> |
| 1                                                                                        | contig000004  | 157,269           | 155,719          | 1551               |
| 2                                                                                        | contig000004  | 152,549           | 150,963          | 1587               |
| 3                                                                                        | contig000033  | 8187              | 6544             | 1644               |
| <b>Acyl-CoA Dehydrogenase (EC 1.3.8.1) (EC 1.3.8.7) (Putative)</b>                       |               |                   |                  |                    |
|                                                                                          | <b>Contig</b> | <b>Start (bp)</b> | <b>Stop (bp)</b> | <b>Length (bp)</b> |
| 1                                                                                        | contig000016  | 19,917            | 20,870           | 954                |
| 2                                                                                        | contig000016  | 24,758            | 23,676           | 1083               |
| 3                                                                                        | contig000038  | 54,006            | 55,709           | 1704               |
| 4                                                                                        | contig000038  | 55,738            | 57,438           | 1701               |
| 5                                                                                        | contig000063  | 22,059            | 23,198           | 1140               |
| 6                                                                                        | contig000070  | 24,723            | 23,602           | 1122               |
| <b>2,4-dienoyl-CoA Reductase, NADH: Flavin Oxidoreductases, Old Yellow Enzyme Family</b> |               |                   |                  |                    |
|                                                                                          | <b>Contig</b> | <b>Start (bp)</b> | <b>Stop (bp)</b> | <b>Length (bp)</b> |
| 1                                                                                        | contig000070  | 29,836            | 28,598           | 1239               |
| <b>Enoyl-CoA Hydratases (EC 4.2.1.17)</b>                                                |               |                   |                  |                    |
|                                                                                          | <b>Contig</b> | <b>Start (bp)</b> | <b>Stop (bp)</b> | <b>Length (bp)</b> |
| 1                                                                                        | contig000004  | 157,510           | 158,325          | 816                |
| 2                                                                                        | contig000008  | 7568              | 6855             | 711                |
| 3                                                                                        | contig000008  | 11,332            | 12,129           | 798                |
| 4                                                                                        | contig000013  | 81,498            | 80,584           | 915                |
| 5                                                                                        | contig000014  | 109,166           | 109,984          | 819                |
| 6                                                                                        | contig000016  | 7177              | 8541             | 1365               |
| 7                                                                                        | contig000016  | 14,015            | 13,206           | 810                |
| 8                                                                                        | contig000029  | 64,705            | 66,807           | 2103               |
| 9                                                                                        | contig000030  | 66,724            | 65,951           | 774                |
| 10                                                                                       | contig000034  | 65,180            | 64,380           | 801                |
| 11                                                                                       | contig000049  | 15,615            | 14,776           | 840                |
| 12                                                                                       | contig000066  | 20,230            | 20,994           | 765                |
| 13                                                                                       | contig000084  | 24,228            | 25,004           | 777                |
| 14                                                                                       | contig000113  | 12,043            | 11,240           | 804                |
| <b>3-hydroxyacyl-CoA Dehydrogenases (EC 1.1.1.35)</b>                                    |               |                   |                  |                    |
|                                                                                          | <b>Contig</b> | <b>Start (bp)</b> | <b>Stop (bp)</b> | <b>Length (bp)</b> |
| 1                                                                                        | contig000001  | 58,250            | 56,769           | 1482               |
| 2                                                                                        | contig000008  | 27,541            | 26,771           | 771                |
| 3                                                                                        | contig000008  | 35,830            | 36,684           | 855                |
| 4                                                                                        | contig000016  | 5912              | 5157             | 756                |
| 5                                                                                        | contig000029  | 64,705            | 66,807           | 2103               |
| 6                                                                                        | contig000628  | 289               | 86               | 204                |

| 3-ketoacyl-CoA Thiolase (EC 2.3.1.16) |              |            |           |             |
|---------------------------------------|--------------|------------|-----------|-------------|
|                                       | Contig       | Start (bp) | Stop (bp) | Length (bp) |
| 1                                     | contig000001 | 49,954     | 48,761    | 1194        |
| 2                                     | contig000002 | 54,042     | 52,825    | 1218        |
| 3                                     | contig000005 | 108,324    | 109,448   | 1125        |
| 4                                     | contig000008 | 19,025     | 17,337    | 1689        |
| 5                                     | contig000008 | 34,593     | 35,762    | 1170        |
| 6                                     | contig000008 | 70,364     | 69,177    | 1188        |
| 7                                     | contig000009 | 12,987     | 11,806    | 1182        |
| 8                                     | contig000025 | 61,696     | 62,844    | 1149        |
| 9                                     | contig000029 | 63,524     | 64,708    | 1185        |
| 10                                    | contig000033 | 3101       | 1878      | 1224        |
| 11                                    | contig000033 | 6551       | 5379      | 1173        |
| 12                                    | contig000034 | 68,356     | 67,148    | 1209        |
| 13                                    | contig000049 | 17,108     | 18,265    | 1158        |
| 14                                    | contig000066 | 45,751     | 46,896    | 1146        |
| 15                                    | contig000090 | 24,745     | 23,573    | 1173        |

| $\alpha$ -Methylacyl-CoA Racemase (Mcr) (EC 5.1.99.4) |              |            |           |             |
|-------------------------------------------------------|--------------|------------|-----------|-------------|
|                                                       | Contig       | Start (bp) | Stop (bp) | Length (bp) |
| 1                                                     | contig000016 | 8557       | 9753      | 1194        |
| 2                                                     | contig000016 | 110,010    | 111,122   | 1113        |
| 3                                                     | contig000032 | 61,506     | 60,388    | 1119        |

| Superoxide Dismutase |              |            |           |             |
|----------------------|--------------|------------|-----------|-------------|
|                      | Contig       | Start (bp) | Stop (bp) | Length (bp) |
| 1                    | contig000020 | 73,292     | 72,687    | 606         |
| 2                    | contig000056 | 23,468     | 23,869    | 402         |

Appendix B



Figure A2. Cluster of Orthologous (COGs) for Dactylosporangium sp. AC04546 analyzed using egg-NOG mapper v.2 [42]. CELLULAR PROCESSES AND SIGNALING [D] Cell cycle control, cell

division, chromosome partitioning, [M] Cell wall/membrane/envelope biogenesis, [N] Cell motility; [O] Post-translational modification, protein turnover, and chaperones, [T] Signal transduction mechanisms, [U] Intracellular trafficking, secretion, and vesicular transport, [V] Defense mechanisms [W] Extracellular structures, [Y] Nuclear structure, [Z] Cytoskeleton; INFORMATION STORAGE AND PROCESSING [A] RNA processing and modification, [B] Chromatin structure and dynamics, [J] Translation, ribosomal structure and biogenesis, [K] Transcription, [L] Replication, recombination and repair; METABOLISM [C] Energy production and conversion, [E] Amino acid transport and metabolism, [F] Nucleotide transport and metabolism, [G] Carbohydrate transport and metabolism, [H] Coenzyme transport and metabolism, [I] Lipid transport and metabolism, [P] Inorganic ion transport and metabolism, [Q] Secondary metabolites biosynthesis, transport, and catabolism; POORLY CHARACTERIZED [R] General function prediction only, [S] Function unknown.

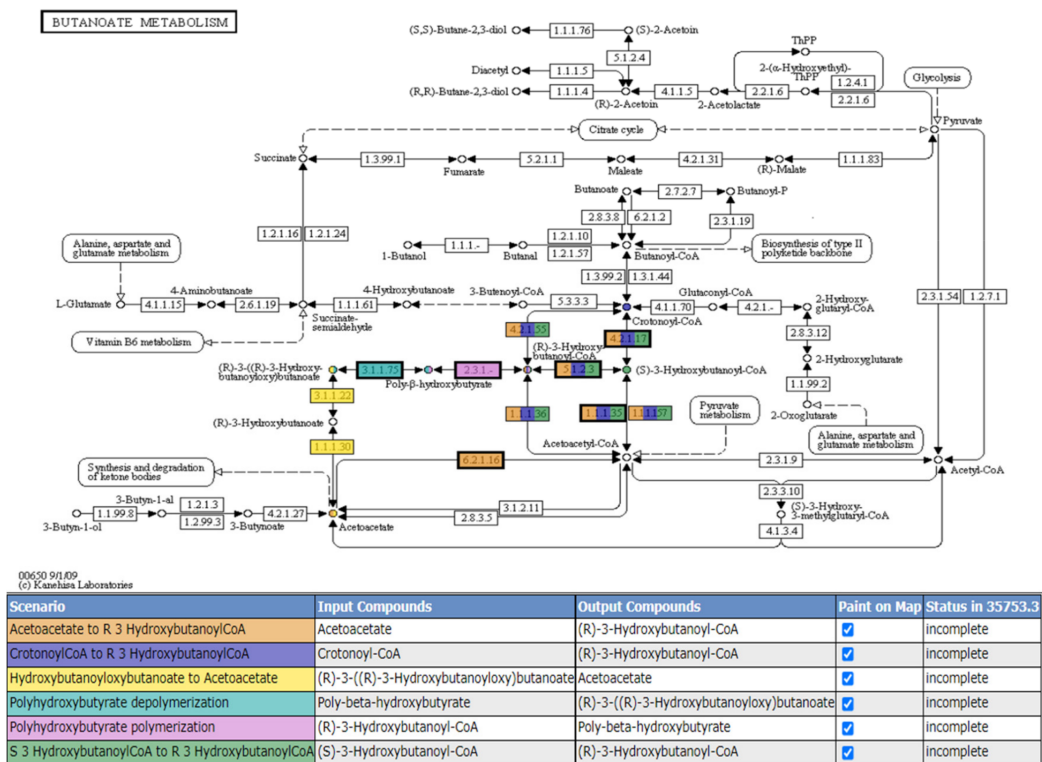


Figure A3. *Dactylosporangium* sp. AC04546 polyhydroxybutyrate metabolism subsystem based on KEGG pathway, predicted by RAST server, and viewed using The SEED Viewer. Color on the MAP corresponds to the predicted scenario in the legend below.

Table A7. *Dactylosporangium* sp. AC04546 CRISPR array detected using CRISPRFinder server.

|    | Contig        | Start (bp) | Stop (bp) |
|----|---------------|------------|-----------|
| 1  | Contig000003  | 116,444    | 121,041   |
| 2  | Contig000003  | 136,865    | 140,549   |
| 3  | Contig000003  | 140,628    | 140,897   |
| 4  | Contig000003  | 140,978    | 141,433   |
| 5  | Contig000003  | 158,732    | 160,550   |
| 6  | Contig000003  | 167,167    | 169,203   |
| 7  | Contig 000002 | 176,434    | 176,695   |
| 8  | Contig000031  | 68,133     | 68,314    |
| 9  | Contig000051  | 75,685     | 76,012    |
| 10 | Contig000103  | 11,150     | 11,388    |
| 11 | Contig000106  | 41,651     | 41,808    |

**Table A8.** *Dactylosporangium* sp. AC04546 antibiotic resistant genes identified from CARD database.

|   | Contig       | Start (bp) | Stop (bp) | Length (bp) | Classification                        | Identity (%) |
|---|--------------|------------|-----------|-------------|---------------------------------------|--------------|
| 1 | Contig000013 | 85,766     | 85,392    | 375         | aminoglycoside (ARO:3003395)          | 83           |
| 2 | Contig000013 | 82,643     | 81,450    | 1194        | glycopeptide antibiotic (ARO:3005036) | 89           |

**Table A9.** *Dactylosporangium* sp. AC04546 drug target gene identified using PATRIC server, verified using DrugBank server.

|   | Contig      | Product                          | Start (bp) | Stop (bp) | Length (bp) | Query Coverage | Identity (%) |
|---|-------------|----------------------------------|------------|-----------|-------------|----------------|--------------|
| 1 | contig00024 | Cell division protein FtsZ, ftsZ | 41,193     | 42,296    | 386         | 85             | 83           |
| 2 | contig00121 | RecA protein, recA               | 1566       | 517       | 1050        | 93             | 88           |

**Table A10.** *Dactylosporangium* sp. AC04546 urease and urea transporter putative genes identified using RAST server.

|    | Contig       | Start (bp) | Stop (bp) | Length (bp) | Function                                             |
|----|--------------|------------|-----------|-------------|------------------------------------------------------|
| 1  | contig000144 | 11,078     | 11,380    | 303         | Urease gamma subunit (EC 3.5.1.5) UreA               |
| 2  | contig000144 | 11,377     | 11,682    | 306         | Urease beta subunit (EC 3.5.1.5) UreB                |
| 3  | contig000144 | 11,679     | 13,388    | 1710        | Urease alpha subunit (EC 3.5.1.5) UreC               |
| 4  | contig000144 | 13,391     | 14,050    | 660         | Urease accessory protein UreF                        |
| 5  | contig000144 | 13,391     | 14,050    | 660         | Urease accessory protein UreF                        |
| 6  | contig000144 | 13,391     | 14,050    | 660         | Urease accessory protein UreF                        |
| 7  | contig000144 | 14,040     | 14,738    | 699         | Urease accessory protein UreG                        |
| 8  | contig000144 | 14,040     | 14,738    | 699         | Urease accessory protein UreG                        |
| 9  | contig000144 | 14,735     | 15,394    | 660         | Urease accessory protein UreD                        |
| 10 | contig000144 | 14,735     | 15,394    | 660         | Urease accessory protein UreD                        |
| 11 | contig000003 | 213,232    | 214,527   | 1296        | Urea ABC transporter, substrate-binding protein UrtA |
| 12 | contig000003 | 214,640    | 215,524   | 885         | Urea ABC transporter, permease protein UrtB          |
| 13 | contig000003 | 215,521    | 216,615   | 1095        | Urea ABC transporter, permease protein UrtC          |
| 14 | contig000003 | 216,612    | 217,448   | 837         | Urea ABC transporter, ATPase protein UrtD            |
| 15 | contig000003 | 217,450    | 218,133   | 684         | Urea ABC transporter, ATPase protein UrtE            |
| 16 | contig000174 | 8890       | 9240      | 351         | Urea ABC transporter, ATPase protein UrtE            |

**Table A11.** *Dactylosporangium* sp. AC04546 secondary metabolite biosynthetic gene clusters (BGCs) were predicted using AntiSMASH 6.0.

| Region       | Type                   | From    | To      | Most Similar Known Cluster                  | Similarity                                       |
|--------------|------------------------|---------|---------|---------------------------------------------|--------------------------------------------------|
| Region 7.1   | other                  | 1       | 32,122  |                                             |                                                  |
| Region 7.2   | butyrolactone          | 181,275 | 189,513 | colabomycin E                               | Polyketide:Type II                               |
| Region 9.1   | betalactone            | 127,964 | 156,777 |                                             | 4%                                               |
| Region 23.1  | LAP                    | 63,471  | 86,862  |                                             |                                                  |
| Region 28.1  | terpene                | 63,486  | 89,541  | hopene                                      | Terpene                                          |
| Region 29.1  | NRPS                   | 1       | 53,614  | gobichelin A/gobichelin B                   | NRP                                              |
| Region 33.1  | redox-cofactor         | 47,552  | 69,629  | lankacidin C                                | NRP + Polyketide                                 |
| Region 38.1  | lanthipeptide-class-iv | 1       | 17,570  | salinilactam                                | Polyketide                                       |
| Region 47.1  | RiPP-like              | 1       | 5832    |                                             |                                                  |
| Region 52.1  | thioamide-NRP          | 23,205  | 83,117  | netropsin                                   | NRP                                              |
| Region 58.1  | redox-cofactor         | 54,961  | 76,748  |                                             | 27%                                              |
| Region 62.1  | NAPAA                  | 27,298  | 61,263  |                                             |                                                  |
| Region 79.1  | terpene                | 39,001  | 58,687  | isorenieratene                              | Terpene                                          |
| Region 81.1  | lassopeptide           | 19,124  | 41,635  | siamycin I                                  | RiPP                                             |
| Region 87.1  | T2PKS                  | 1       | 51,425  | arenimycin A                                | Polyketide:Type II + Saccharide:Hybrid/tailoring |
| Region 90.1  | terpene                | 35,800  | 49,030  | calicheamicin                               | Polyketide                                       |
| Region 99.1  | T3PKS                  | 20,966  | 45,958  | alkyl-O-dihydrogeranyl-methoxyhydroquinones | Terpene + Polyketide                             |
| Region 118.1 | NRPS                   | 8823    | 36,925  | A54145                                      | NRP                                              |
| Region 229.1 | siderophore            | 253     | 6171    |                                             | 3%                                               |

Region, contig of the draft genome; NRPS, Non-ribosomal peptide synthetase cluster; RiPP, ribosomally synthesized and post-translationally modified peptide product (RiPP) cluster; RRE-containing, RRE-element containing cluster; saccharide, Saccharide cluster (loose strictness, likely from primary metabolism); T1PKS, Type I PKS (Polyketide synthase); T2PKS, Type II PKS; T3PKS, Type III PKS.

**Table A12.** Distribution and loci of  $\beta$ -oxidation related putative genes in the draft genome of *Dactylosporangium* sp. AC04546.

| <b>Twin-Arginine Translocation Protein, TAT Protein (TatA, TatB, TatC)</b>   |               |                   |                  |                    |
|------------------------------------------------------------------------------|---------------|-------------------|------------------|--------------------|
|                                                                              | <b>Contig</b> | <b>Start (bp)</b> | <b>Stop (bp)</b> | <b>Length (bp)</b> |
| 1                                                                            | contig000009  | 102,753           | 102,487          | 267                |
| 2                                                                            | contig000071  | 21,417            | 20,446           | 972                |
| 3                                                                            | contig000071  | 21,698            | 21,432           | 267                |
| 4                                                                            | contig000128  | 29,800            | 29,369           | 432                |
| <b>Acyl-CoA Synthase (EC 6.2.1.1)</b>                                        |               |                   |                  |                    |
|                                                                              | <b>Contig</b> | <b>Start (bp)</b> | <b>Stop (bp)</b> | <b>Length (bp)</b> |
| 1                                                                            | contig000098  | 31,823            | 33,694           | 1872               |
| 2                                                                            | contig000151  | 21,809            | 19,845           | 1965               |
| <b>Transcriptional Regulator, TetR Family on the Same Contig as lcp Gene</b> |               |                   |                  |                    |
|                                                                              | <b>Contig</b> | <b>Start (bp)</b> | <b>Stop (bp)</b> | <b>Length (bp)</b> |
| 1                                                                            | contig000001  | 362,871           | 363,434          | 564                |
| 2                                                                            | contig000082  | 7433              | 8032             | 600                |
| 3                                                                            | contig000082  | 41,434            | 40,763           | 672                |
| 4                                                                            | contig000082  | 43,443            | 42,790           | 654                |
| <b>Acyl-CoA Dehydrogenase (EC 1.3.8.1) (EC 1.3.8.8) (Putative)</b>           |               |                   |                  |                    |
|                                                                              | <b>Contig</b> | <b>Start (bp)</b> | <b>Stop (bp)</b> | <b>Length (bp)</b> |
|                                                                              | contig000001  | 308,373           | 309,527          | 1155               |
|                                                                              | contig000002  | 210,799           | 211,995          | 1197               |
|                                                                              | contig000002  | 226,160           | 224,997          | 1164               |
|                                                                              | contig000006  | 79,214            | 80,359           | 1146               |
|                                                                              | contig000006  | 91,911            | 93,056           | 1146               |
|                                                                              | contig000006  | 109,177           | 110,382          | 1206               |
|                                                                              | contig000006  | 123,342           | 124,502          | 1161               |
|                                                                              | contig000007  | 32,267            | 31,008           | 1260               |
|                                                                              | contig000007  | 42,815            | 43,978           | 1164               |
|                                                                              | contig000008  | 111,357           | 112,454          | 1098               |
|                                                                              | contig000009  | 125,869           | 124,712          | 1158               |
|                                                                              | contig000010  | 136,785           | 135,604          | 1182               |
|                                                                              | contig000010  | 151,583           | 150,426          | 1158               |
|                                                                              | contig000015  | 106,328           | 105,189          | 1140               |
|                                                                              | contig000015  | 125,651           | 124,686          | 966                |
|                                                                              | contig000015  | 126,787           | 125,651          | 1137               |
|                                                                              | contig000022  | 41,492            | 42,652           | 1161               |
|                                                                              | contig000026  | 55,545            | 54,331           | 1215               |
|                                                                              | contig000031  | 60,451            | 59,240           | 1212               |
|                                                                              | contig000032  | 93,065            | 91,926           | 1140               |
|                                                                              | contig000039  | 4910              | 3720             | 1191               |
|                                                                              | contig000039  | 26,773            | 27,924           | 1152               |
|                                                                              | contig000043  | 24,574            | 26,259           | 1686               |
|                                                                              | contig000058  | 40,472            | 41,617           | 1146               |
|                                                                              | contig000058  | 44,004            | 45,245           | 1242               |
|                                                                              | contig000070  | 60,103            | 61,281           | 1179               |
|                                                                              | contig000079  | 56,242            | 57,411           | 1170               |
|                                                                              | contig000079  | 57,408            | 58,457           | 1050               |
|                                                                              | contig000082  | 5300              | 6439             | 1140               |
|                                                                              | contig000082  | 39,644            | 40,777           | 1134               |
|                                                                              | contig000095  | 11,194            | 12,378           | 1185               |
|                                                                              | contig000095  | 12,375            | 13,523           | 1149               |
|                                                                              | contig000102  | 18,437            | 17,304           | 1134               |
|                                                                              | contig000108  | 19,517            | 20,767           | 1251               |
|                                                                              | contig000116  | 8097              | 6244             | 1854               |
|                                                                              | contig000121  | 6633              | 5491             | 1143               |
|                                                                              | contig000128  | 19,042            | 17,828           | 1215               |

Table A12. Cont.

| Acyl-CoA Dehydrogenase (EC 1.3.8.1) (EC 1.3.8.8) (Putative) |              |           |             |      |
|-------------------------------------------------------------|--------------|-----------|-------------|------|
| Contig                                                      | Start (bp)   | Stop (bp) | Length (bp) |      |
| contig000154                                                | 11,134       | 9848      | 1287        |      |
| contig000154                                                | 12,217       | 11,150    | 1068        |      |
| contig000154                                                | 13,405       | 12,230    | 1176        |      |
| contig000157                                                | 3155         | 4306      | 1152        |      |
| contig000202                                                | 7053         | 8201      | 1149        |      |
| contig000218                                                | 2054         | 126       | 1929        |      |
| 2,4-dienoyl-CoA Reductase (EC 1.3.1.34)                     |              |           |             |      |
| Contig                                                      | Start (bp)   | Stop (bp) | Length (bp) |      |
| 1                                                           | contig000007 | 126,818   | 125,733     | 1086 |
| Enoyl-CoA Hydratases (EC 4.2.1.17)                          |              |           |             |      |
| Contig                                                      | Start (bp)   | Stop (bp) | Length (bp) |      |
| 1                                                           | contig000001 | 296,029   | 295,283     | 747  |
| 2                                                           | contig000001 | 300,636   | 301,421     | 786  |
| 3                                                           | contig000001 | 307,165   | 306,362     | 804  |
| 4                                                           | contig000001 | 329,756   | 330,586     | 831  |
| 5                                                           | contig000001 | 344,214   | 344,978     | 765  |
| 6                                                           | contig000002 | 202,945   | 202,163     | 783  |
| 7                                                           | contig000002 | 206,845   | 205,931     | 915  |
| 8                                                           | contig000006 | 81,885    | 81,088      | 798  |
| 9                                                           | contig000006 | 89,484    | 90,293      | 810  |
| 10                                                          | contig000006 | 97,828    | 96,953      | 876  |
| 11                                                          | contig000006 | 114,743   | 11,3946     | 798  |
| 12                                                          | contig000006 | 118,886   | 118,125     | 762  |
| 13                                                          | contig000006 | 120,324   | 122,495     | 2172 |
| 14                                                          | contig000006 | 124,537   | 125,340     | 804  |
| 15                                                          | contig000008 | 131,053   | 131,946     | 894  |
| 16                                                          | contig000009 | 130,569   | 131,345     | 777  |
| 17                                                          | contig000015 | 104,062   | 103,208     | 855  |
| 18                                                          | contig000017 | 101,441   | 100,656     | 786  |
| 19                                                          | contig000019 | 132,075   | 132,860     | 786  |
| 20                                                          | contig000025 | 2819      | 2001        | 819  |
| 21                                                          | contig000025 | 43,741    | 42,917      | 825  |
| 22                                                          | contig000027 | 47,243    | 48,025      | 783  |
| 23                                                          | contig000028 | 22,979    | 23,818      | 840  |
| 24                                                          | contig000028 | 26,480    | 28,549      | 2070 |
| 25                                                          | contig000031 | 14,833    | 12,764      | 2070 |
| 26                                                          | contig000032 | 69,957    | 70,736      | 780  |
| 27                                                          | contig000032 | 90,750    | 89,941      | 810  |
| 28                                                          | contig000039 | 8258      | 8986        | 729  |
| 29                                                          | contig000039 | 12,002    | 11,265      | 738  |
| 30                                                          | contig000039 | 33,697    | 34,668      | 972  |
| 31                                                          | contig000039 | 35,986    | 36,708      | 723  |
| 32                                                          | contig000043 | 48,021    | 50,117      | 2097 |
| 33                                                          | contig000045 | 37,575    | 36,832      | 744  |
| 34                                                          | contig000047 | 5992      | 5237        | 756  |
| 35                                                          | contig000048 | 27,562    | 26,795      | 768  |
| 36                                                          | contig000070 | 58,232    | 59,101      | 870  |
| 37                                                          | contig000070 | 61,278    | 62,096      | 819  |
| 38                                                          | contig000082 | 28,779    | 30,890      | 2112 |
| 39                                                          | contig000095 | 10,175    | 9405        | 771  |
| 40                                                          | contig000095 | 20,285    | 21,049      | 765  |
| 41                                                          | contig000095 | 30,027    | 29,176      | 852  |
| 42                                                          | contig000114 | 7605      | 8369        | 765  |
| 43                                                          | contig000174 | 16,732    | 17,184      | 453  |
| 44                                                          | contig000227 | 3486      | 2695        | 792  |

Table A12. Cont.

| 3-Hydroxyacyl-CoA Dehydrogenases (EC 1.1.1.35)        |              |            |           |             |
|-------------------------------------------------------|--------------|------------|-----------|-------------|
|                                                       | Contig       | Start (bp) | Stop (bp) | Length (bp) |
| 1                                                     | contig000017 | 39,722     | 41,509    | 1788        |
| 2                                                     | contig000018 | 104,278    | 105,594   | 1317        |
| 3                                                     | contig000095 | 18,898     | 18,137    | 762         |
| 4                                                     | contig000095 | 21,871     | 21,101    | 771         |
| Thiolase/3-Ketoacyl-CoA Thiolase (EC 2.3.1.16)        |              |            |           |             |
|                                                       | Contig       | Start (bp) | Stop (bp) | Length (bp) |
| 1                                                     | contig000001 | 189,682    | 190,872   | 1191        |
| 2                                                     | contig000001 | 318,428    | 317,205   | 1224        |
| 3                                                     | contig000001 | 337,505    | 336,360   | 1146        |
| 4                                                     | contig000006 | 78,027     | 79,214    | 1188        |
| 5                                                     | contig000006 | 119,071    | 120,294   | 1224        |
| 6                                                     | contig000015 | 116,318    | 115,128   | 1191        |
| 7                                                     | contig000015 | 118,590    | 119,738   | 1149        |
| 8                                                     | contig000017 | 68,346     | 69,533    | 1188        |
| 9                                                     | contig000018 | 104,185    | 102,911   | 1275        |
| 10                                                    | contig000027 | 53,803     | 54,987    | 1185        |
| 11                                                    | contig000028 | 25,272     | 26,474    | 1203        |
| 12                                                    | contig000031 | 16,023     | 14,830    | 1194        |
| 13                                                    | contig000032 | 86,429     | 85,236    | 1194        |
| 14                                                    | contig000032 | 97,872     | 95,914    | 1959        |
| 15                                                    | contig000043 | 46,807     | 48,018    | 1212        |
| 16                                                    | contig000058 | 45,434     | 46,648    | 1215        |
| 17                                                    | contig000082 | 27,565     | 28,776    | 1212        |
| 18                                                    | contig000095 | 20,128     | 18,941    | 1188        |
| 19                                                    | contig000105 | 40,143     | 38,899    | 1245        |
| 20                                                    | contig000007 | 41,311     | 42,423    | 1113        |
| 21                                                    | contig000039 | 18,566     | 19,750    | 1185        |
| $\alpha$ -Methylacyl-CoA Racemase (Mcr) (EC 5.1.99.4) |              |            |           |             |
|                                                       | Contig       | Start (bp) | Stop (bp) | Length (bp) |
| 1                                                     | contig000001 | 326,963    | 328,114   | 1152        |
| 2                                                     | contig000027 | 43,150     | 41,963    | 1188        |
| 3                                                     | contig000032 | 91,899     | 90,757    | 1143        |
| 4                                                     | contig000082 | 3034       | 1871      | 1164        |
| 5                                                     | contig000095 | 15,365     | 16,525    | 1161        |

## References

- Cornish, K. Alternative natural rubber crops: Why should we care? *Technol. Innov.* **2017**, *18*, 244–255. [CrossRef]
- Blaettler, K.G. The Manufacturing Process of Rubber. 2018. Available online: <https://sciencing.com/manufacturing-process-rubber-5206099.html> (accessed on 23 August 2021).
- Valdés, C.; Hernández, C.; Morales-Vera, R.; Andler, R. Desulfurization of vulcanized rubber particles using biological and couple microwave-chemical methods. *Front. Environ. Sci.* **2021**, *9*, 1–10. [CrossRef]
- Andler, R. Bacterial and enzymatic degradation of poly(*cis*-1,4-isoprene) rubber: Novel biotechnological applications. *Biotechnol. Adv.* **2020**, *44*, 107606. [CrossRef] [PubMed]
- Kasai, D. Poly(*cis*-1,4-isoprene)-cleavage enzymes from natural rubber-utilizing bacteria. *Biosci. Biotechnol. Biochem.* **2020**, *84*, 1089–1097. [CrossRef]
- Spence, D.; Van Niel, C.B. Bacterial decomposition of the rubber in *Hevea* latex. *Ind. Eng. Chem.* **1936**, *28*, 847–850. [CrossRef]
- De Vries, O. Decomposition of rubber hydrocarbons by fungi. *Zentbl. Bakteriol. Parasitenkd. Infekt.* **1928**, *74*, 22–24.
- Shaposhnikov, V.; Rabortnova, I.; Iarmola, G.; Kuznetsova, V.; Mozokhina-Porshniakova, N.N. Destructive effect of bacterial development on natural rubber. *Mikrobiologiya* **1952**, *21*, 47–54.
- Röther, W.; Birke, J.; Grond, S.; Beltran, J.M.; Jendrosseck, D. Production of functionalized oligo-isoprenoids by enzymatic cleavage of rubber. *Microb. Biotechnol.* **2017**, *10*, 1426–1433. [CrossRef]

10. Hiessl, S.; Schuldes, J.; Thürmer, A.; Halbsguth, T.; Bröker, D.; Angelov, A.; Liebl, W.; Daniel, R.; Steinbüchel, A. Involvement of two latex-clearing proteins during rubber degradation and insights into the subsequent degradation pathway revealed by the genome sequence of *Gordonia polyisoprenivorans* strain VH2. *Appl. Environ. Microbiol.* **2012**, *78*, 2874–2887. [CrossRef]
11. Andler, R.; Vivod, R.; Steinbüchel, A. Synthesis of polyhydroxyalkanoates through the biodegradation of poly(*cis*-1,4-isoprene) rubber. *J. Biosci. Bioeng.* **2019**, *127*, 360–365. [CrossRef]
12. Tsuchii, A.; Suzuki, T.; Takeda, K. Microbial degradation of natural rubber vulcanizates. *Appl. Environ. Microbiol.* **1985**, *50*, 965–970. [CrossRef]
13. Azadi, D.; Shojaei, H.; Mobasherizadeh, S.; Naser, A.D. Screening, isolation and molecular identification of biodegrading mycobacteria from Iranian ecosystems and analysis of their biodegradation activity. *AMB Express* **2017**, *7*, 180. [CrossRef]
14. Goodfellow, M.; Williams, S.T. Ecology of actinomycetes. *Annu. Rev. Microbiol.* **1983**, *37*, 189–216. [CrossRef]
15. Manurung, R.; Abdullah, Z.C.; Ahmad, F.B.; Kuek, C. Biodiversity-biotechnology: Gateway to discoveries. In Proceedings of the Sustainable Utilization and Wealth Creation, Kuching, Sarawak, Malaysia, 19–21 November 2008.
16. Hassan, Q.P.; Bhat, A.M.; Shah, A.M. Chapter 6: Bioprospecting actinobacteria for bioactive secondary metabolites from untapped ecoregions of the Northwestern Himalayas. In *New and Future Developments in Microbial Biotechnology and Bioengineering: Microbial Secondary Metabolites Biochemistry and Applications*; Elsevier: Amsterdam, The Netherlands, 2019; pp. 77–85. Available online: <https://doi.org/10.1016/B978-0-444-63504-4.00006-2> (accessed on 25 August 2021).
17. Clark, T. Enhancing the biodegradation of waste rubber discarded rubber materials. In Proceedings of the International Latex Conference, Fairlawn, OH, USA; 2015. Available online: <https://www.rubbernews.com/assets/PDF/RN10077285.PDF> (accessed on 24 July 2020).
18. Chengalroyen, M.D.; Dabbs, E.R. The biodegradation of latex rubber: A minireview. *J. Polym. Environ.* **2013**, *21*, 874–880. [CrossRef]
19. Shivlata, L.; Satyanarayana, T. Thermophilic and alkaliphilic actinobacteria: Biology and potential applications. *Front. Microbiol.* **2015**, *6*, 1014. [CrossRef]
20. Linh, D.V.; Huong, L.N.; Tabata, M.; Imai, S.; Iijima, S.; Kasai, D.; Anh, T.K.; Fukuda, M. Characterization and functional expression of a rubber degradation gene of a *Nocardia* degrader from a rubber-processing factory. *J. Biosci. Bioeng.* **2017**, *123*, 412–418. [CrossRef]
21. Jendrossek, D.; Tomasi, G.; Kroppenstedt, R.M. Bacterial degradation of natural rubber: A privilege of actinomycetes? *FEMS Microbiol. Lett.* **1997**, *150*, 179–188. [CrossRef]
22. Vivod, R.; Andler, R.; Oetermann, S.; Altenhoff, A.L.; Seipel, N.; Holtkamp, M.; Hogeback, J.; Karst, U.; Steinbüchel, A. Characterization of the latex clearing protein of the poly(*cis*-1,4-isoprene) and poly(*trans*-1,4-isoprene) degrading bacterium *Nocardia nova* SH22a. *J. Gen. Appl. Microbiol.* **2019**, *65*, 293–300. [CrossRef]
23. Luo, Q.; Hiessl, S.; Poehlein, A.; Daniel, R.; Steinbüchel, A. Insights into the microbial degradation of rubber and gutta-percha by analysis of the complete genome of *Nocardia nova* SH22a. *Appl. Environ. Microbiol.* **2014**, *80*, 3895–3907. [CrossRef]
24. Watcharakul, S.; Röther, W.; Birke, J.; Umsakul, K.; Hodgson, B.; Jendrossek, D. Biochemical and spectroscopic characterization of purified latex clearing protein (Lcp) from newly isolated rubber degrading *Rhodococcus rhodochrous* strain RPK1 reveals novel properties of Lcp. *BMC Microbiol.* **2016**, *16*, 92. [CrossRef]
25. Nawong, C.; Umsakul, K.; Sermwittayawong, N. Rubber gloves biodegradation by a consortium, mixed culture and pure culture isolated from soil samples. *Braz. J. Microbiol.* **2018**, *49*, 481–488. [CrossRef] [PubMed]
26. Akkharabunditsakul, V.; Tanrattanakul, V.; Umsakul, K. Biodegradation of synthetic rubbers by a mixed culture isolated from various rubber factory soils in Songkhla, Thailand. *Int. J. Adv. Agric. Environ. Eng.* **2017**, *4*, 33–37.
27. Parte, A.C. LPSN-list of prokaryotic names with standing in nomenclature. *Nucleic Acids Res.* **2018**, *42*, D613–D616. [CrossRef] [PubMed]
28. Braaz, R.; Fischer, P.; Jendrossek, D. Novel type of Heme-dependent oxygenase catalyzes oxidative Cleavage of rubber (poly-*cis*-1,4-isoprene). *Appl. Environ. Microbiol.* **2004**, *70*, 7388–7395. [CrossRef]
29. Chia, K.-H.; Nanthini, J.; Thottathil, G.P.; Najimudin, N.; Haris, M.R.H.M.; Sudesh, K. Identification of new rubber-degrading bacterial strains from aged latex. *Polym. Degrad. Stab.* **2014**, *109*, 354–361. [CrossRef]
30. Heisey, R.M.; Papadatos, S. Isolation of microorganisms able to metabolize purified natural rubber. *Appl. Environ. Microbiol.* **1995**, *61*, 3092–3097. [CrossRef]
31. Shirling, E.B.; Gottlieb, D. Methods for characterization of *Streptomyces* species. *Int. J. Syst. Bacteriol.* **1966**, *16*, 340. [CrossRef]
32. Hamaki, T.; Suzuki, M.; Fudou, R.; Jojima, Y.; Kajjura, T.; Tabuchi, A.; Sen, K.; Shibai, H. Isolation of novel bacteria and actinomycetes using soil-extract agar medium. *J. Biosci. Bioeng.* **2005**, *99*, 485–492. [CrossRef]
33. *Applied Biosystems, Sequence Scanner*; Thermo Fisher Scientific: Waltham, MA, USA. Available online: <https://www.thermofisher.cn/cn/zh/home.html> (accessed on 5 August 2021).
34. Hall, T.A. BioEdit: A user-friendly biological sequence alignment editor and analysis program for Windows 95/98/NT. *Nucleic Acid Symp. Ser.* **1999**, *41*, 95–98.
35. Kumar, S.; Stecher, G.; Li, M.; Nnyaz, C.; Tamura, K. MEGA X: Molecular evolutionary genetics analysis across computing platforms. *Mol. Biol. Evol.* **2018**, *35*, 1547–1549. [CrossRef]
36. Bateman, A.; Bridge, A.; Wu, C. UniProt. UniProt Consortium (Online). Available online: <https://www.uniprot.org/blast/> (accessed on 5 August 2021).

37. Gasteiger, E.; Gattiker, A.; Hoogland, C.; Ivanyi, I.; Appel, R.D.; Bairoch, A. ExpPASy: The proteomics server for in-depth protein knowledge and analysis. *Nucleic Acids Res.* **2003**, *31*, 3784–3788. [[CrossRef](#)]
38. Moore, E.; Arnscheidt, A.; Krüger, A.; Strömpl, C.; Mau, M. Section 1 update: Simplified protocols for the preparation of genomic DNA from bacterial cultures. *Mol. Microb. Ecol. Man.* **2008**. [[CrossRef](#)]
39. Aziz, R.K.; Bartels, D.; Best, A.A.; DeJongh, M.; Disz, T.; Edwards, R.A.; Formsma, K.; Gerdes, S.; Glass, E.M.; Kubal, M.; et al. The RAST server: Rapid annotations using subsystems technology. *BMC Genom.* **2008**, *9*, 75. [[CrossRef](#)]
40. Davis, J.J.; Wattam, A.R.; Aziz, R.K.; Brettin, T.; Butler, R.; Butler, R.M.; Chlenski, P.; Conrad, N.; Dickerman, A.; Dietrich, E.M.; et al. The PATRIC bioinformatics resource center: Expanding data and analysis capabilities. *Nucleic Acids Res.* **2020**, *48*, D606–D612. [[CrossRef](#)]
41. Li, W.; O'Neill, K.R.; Haft, D.H.; DiCuccio, M.; Chetvermin, V.; Badretdin, A.; Coulouris, G.; Chitsaz, F.; Derbyshire, M.K.; Durkin, A.S.; et al. RefSeq: Expanding the prokaryotic genome annotation pipeline reach with protein family model curation. *Nucleic Acids Res.* **2020**, *49*, 1020–1028. [[CrossRef](#)]
42. Cantalapedra, C.P.; Hernández-Plaza, A.; Letunic, I.; Huerta-Cepas, J. EggNOG-mapper v2: Functional annotation, orthology assignments, and domain prediction at the metagenomic scale. *bioRxiv* **2021**. [[CrossRef](#)]
43. Tatusov, R.L.; Galperin, M.Y.; Natale, D.A.; Koonin, E.V. The COG database: A tool for genome-scale analysis of protein functions and evolution. *Nucleic Acids Res.* **2000**, *28*, 33–36. [[CrossRef](#)]
44. Kanehisa, M.; Sato, Y.; Kawashima, M.; Furumichi, M.; Tanabe, M. KEGG as a reference resource for gene and protein annotation. *Nucleic Acids Res.* **2015**, *44*, 457–462. [[CrossRef](#)]
45. Grissa, I.; Vergnaud, G.; Pourcel, C. CRISPRFinder: A web tool to identify clustered regularly interspaced short palindromic repeats. *Nucleic Acids Res.* **2007**, *35*, 52–57. [[CrossRef](#)]
46. Alcock, B.P.; Raphenya, A.R.; Lau, T.T.; Tsang, K.K.; Bouchard, M.; Edalatmand, A.; Huynh, W.; Nguyen, A.L.; Cheng, A.A.; Liu, S.; et al. CARD: Antibiotic resistome surveillance with the comprehensive antibiotic resistance database. *Nucleic Acids Res.* **2020**, *48*, D517–D525.
47. Wishart, D.S.; Feunang, Y.D.; Guo, A.C.; Lo, E.J.; Marcu, A.; Grant, J.R.; Sajed, T.; Johnson, D.; Li, C.; Sayeeda, Z.; et al. DrugBank 5.0: A major update to the DrugBank database for 2018. *Nucleic Acids Res.* **2018**, *46*, D1074–D1082. [[CrossRef](#)]
48. Blin, K.; Shaw, S.; Kloosterman, A.M.; Charlop-Powers, Z.; van Wezel, G.P.; Medema, M.H.; Weber, T. AntiSMASH 6.0: Improving cluster detection and comparison capabilities. *Nucleic Acids Res.* **2021**, *49*, W29–W35. [[CrossRef](#)]
49. Overbeek, R.; Olson, R.; Pusch, G.D.; Olsen, G.J.; Davis, J.J.; Disz, T.; Edwards, R.A.; Gerdes, S.; Parrello, B.; Shukla, M.; et al. The SEED and the rapid annotation of microbial genomes using subsystems technology (RAST). *Nucleic Acid Symp. Ser.* **2013**, *42*, D206–D214. [[CrossRef](#)]
50. UniProt: The universal protein knowledgebase in 2021. *Nucleic Acids Res.* **2021**, *49*, D480–D489. [[CrossRef](#)]
51. Bendtsen, J.D.; Nielsen, H.; Widdick, D.; Palmer, T.; Brunak, S. Prediction of twin-arginine signal peptides. *BMC Bioinform.* **2005**, *6*, 167. [[CrossRef](#)]
52. Arkin, A.P.; Cottingham, R.W.; Henry, C.S.; Harris, N.L.; Stevens, R.L.; Maslov, S.; Dehal, P.; Ware, D.; Perez, F.; Canon, S.; et al. KBase: The United States Department of Energy Systems Biology Knowledgebase. *Nat. Biotechnol.* **2018**, *36*, 566–569. [[CrossRef](#)]
53. Meier-Kolthoff, J.P.; Göker, M. TYGS is an automated high-throughput platform for state-of-the-art genome-based taxonomy. *Nat. Commun.* **2019**, *10*, 2182. [[CrossRef](#)]
54. Auch, A.F.; Klenk, H.P.; Göker, M. Standard operating procedure for calculating genome-to-genome distances based on high-scoring segment pairs. *Stand. Genomic Sci.* **2010**, *2*, 142–148. [[CrossRef](#)]
55. Hördt, A.; López, M.G.; Meier-Kolthoff, J.P.; Schleuning, M.; Weinhold, L.M.; Tindall, B.; Gronow, S.; Kyrpides, N.C.; Woyke, T.; Göker, M. Analysis of 1000+ type-strain genomes substantially improves taxonomic classification of Alphaproteobacteria. *Front. Bioeng. Biotechnol.* **2020**, *11*, 468.
56. Berekaa, M.M.; Linos, A.; Reichelt, R.; Keller, U.; Steinbüchel, A. Effect of pretreatment of rubber material on its biodegradability by various rubber degrading bacteria. *FEMS Microbiol. Lett.* **2000**, *184*, 199–206. [[CrossRef](#)]
57. Basik, A.A.; Juboi, H.; Shamsul, S.S.G.; Sanglier, J.J.; Yeo, T.C. Actinomycetes isolated from Wetland and Hill Paddy during the warm and cool Seasons in Sarawak, East Malaysia. *J. Microbiol. Biotechnol. Food Sci.* **2020**, *9*, 774–781.
58. Rose, K.; Tenberge, K.B.; Steinbüchel, A. Identification and characterization of genes from *Streptomyces* sp. strain K30 responsible for clear zone formation on natural rubber latex and poly(*cis*-1,4-isoprene) rubber degradation. *Biomacromolecules* **2005**, *6*, 180–188. [[CrossRef](#)] [[PubMed](#)]
59. Röther, W.; Austen, S.; Birke, J.; Jendrossek, D. Molecular insights in the cleavage of rubber by the latex-clearing- protein (*Lcp*) of *Streptomyces* sp. strain K30. *Appl. Environ. Microbiol.* **2016**, *82*, 6593–6602. [[CrossRef](#)] [[PubMed](#)]
60. Kim, M.; Oh, H.S.; Park, S.C.; Chun, J. Towards a taxonomic coherence between average nucleotide identity and 16S rRNA gene sequence similarity for species demarcation of prokaryotes. *Int. J. Syst. Evol. Microbiol.* **2014**, *64*, 346–351. [[CrossRef](#)]
61. Volpiano, C.G.; Sant'Anna, F.H.; Ambrosini, A.; de São José, J.F.; Beneduzi, A.; Whitman, W.B.; de Souza, E.M.; Lisboa, B.B.; Vargas, L.K.; Passaglia, L.M. Genomic metrics applied to *Rhizobiales* (Hyphomicrobiales): Species reclassification, identification of unauthentic genomes and false type strains. *Front. Microbiol.* **2021**, *12*, 734850. [[CrossRef](#)]
62. Farris, J.S. Estimating phylogenetic trees from distance matrices. *Am. Nat.* **1972**, *106*, 645–667. [[CrossRef](#)]
63. Wang, B.; Huang, C.; Zhao, H.; Benkovic, S.J. Unraveling the iterative type I polyketide synthases hidden in *Streptomyces*. *Proc. Natl. Acad. Sci. USA* **2020**, *117*, 8449–8454. [[CrossRef](#)]

64. Tsuchii, A.; Takeda, K. Rubber-degrading enzyme from a bacterial culture. *Appl. Environ. Microbiol.* **1990**, *56*, 269–274. [[CrossRef](#)]
65. Rose, K.; Steinbüchel, A. Biodegradation of natural rubber and related compounds: Recent insights into a hardly understood catabolic capability of microorganisms. *Appl. Environ. Microbiol.* **2005**, *71*, 2803–2812. [[CrossRef](#)]
66. Bode, H.B.; Zeeck, A.; Pluckhahn, K.; Jendrossek, D. Physiological and chemical investigations into microbial degradation of synthetic poly(*cis*-1,4-isoprene). *Appl. Environ. Microbiol.* **2000**, *66*, 3680–3685. [[CrossRef](#)]
67. Hiessl, S.; Böse, D.; Oetermann, S.; Eggers, J.; Pietruszka, J.; Steinbüchel, A. Latex clearing protein—An oxygenase cleaving poly(*cis*-1,4-isoprene) rubber at the *cis* double bonds. *Appl. Environ. Microbiol.* **2014**, *80*, 5231–5240. [[CrossRef](#)]
68. Sharma, V.; Siedenbueg, G.; Birke, J.; Mobeen, F.; Jendrossek, D.; Prakash, T. Metabolic and taxonomic insights into the gram-negative natural rubber degrading bacterium *Steroidobacter cummioxidans* sp. nov., strain 35Y. *PLoS ONE* **2018**, *13*, e0200399.
69. Oetermann, S.; Jongasma, R.; Coenen, A.; Keller, J.; Steinbüchel, A. LcpR VH2—Regulating the expression of latex-clearing proteins in *Gordonia polyisoprenivorans* VH2. *Microbiology* **2019**, *165*, 343–354. [[CrossRef](#)]
70. Yikmis, M.; Arenskötter, M.; Rose, K.; Lange, N.; Wernsmann, H.; Wiefel, L.; Steinbüchel, A. Secretion and transcriptional regulation of the latex-clearing protein, Lcp, by the rubber-degrading bacterium *Streptomyces* sp. strain K30. *Appl. Environ. Microbiol.* **2008**, *74*, 5373–5382. [[CrossRef](#)]
71. Coenen, A.; Oetermann, S.; Steinbüchel, A. Identification of LcpRB A3 (2), a novel regulator of Lcp expression in *Streptomyces coelicolor* A3 (2). *Appl. Microbiol. Biotechnol.* **2019**, *103*, 5715–5726. [[CrossRef](#)]
72. Schulte, C.; Arenskötter, M.; Berekaa, M.M.; Arenskötter, Q.; Priefert, H.; Steinbüchel, A. Possible involvement of an extracellular superoxide dismutase (SodA) as a radical scavenger in poly(*cis*-1,4-isoprene) degradation. *Appl. Environ. Microbiol.* **2008**, *74*, 7643–7653. [[CrossRef](#)]
73. Rodriguez-R, L.M.; Konstantinidis, K.T. Bypassing cultivation to identify bacterial species. *Microbe* **2014**, *9*, 111–118. [[CrossRef](#)]
74. Thompson, C.C.; Chimetto, L.; Edwards, R.A.; Swings, J.; Stackebrandt, E.; Thompson, F.L. Microbial genomic taxonomy. *BMC Genom.* **2013**, *14*, 913. [[CrossRef](#)]
75. Behera, B.K.; Chakraborty, H.J.; Patra, B.; Rout, A.K.; Dehury, B.; Das, B.K.; Sarkar, D.J.; Parida, P.K.; Raman, R.K.; Rao, A.R.; et al. Metagenomic analysis reveals bacterial and fungal diversity and their bioremediation potential from sediments of River Ganga and Yamuna in India. *Front. Microbiol.* **2020**, *11*, 2531. [[CrossRef](#)]
76. Elustondo, P.; Zakharian, E.; Pavlov, E. Identification of the polyhydroxybutyrate granules in mammalian cultured cells. *Chem. Biodivers.* **2012**, *9*, 2597–2604. [[CrossRef](#)]
77. Nanthini, J.; Ong, S.Y.; Sudesh, K. Identification of three homologous latex-clearing protein (lcp) genes from the genome of *Streptomyces* sp. strain CFMR 7. *Gene* **2017**, *628*, 146–155. [[CrossRef](#)]
78. Gibu, N.; Arata, T.; Kuboki, S.; Linh, D.V.; Fukuda, M.; Steinbüchel, A.; Kasai, D. Characterization of the genes responsible for rubber degradation in *Actinoplanes* sp. strain OR16. *Appl. Microbiol. Biotechnol.* **2020**, *104*, 7367–7376. [[CrossRef](#)]
79. Nandiyanto, A.B.D.; Oktiani, R.; Ragadhita, R. How to read and interpret FTIR spectroscopy of organic material. *Indones. J. Sci. Technol.* **2019**, *4*, 97–118. [[CrossRef](#)]
80. Birke, J.; Jendrossek, D. Rubber oxygenase and latex clearing protein cleave rubber to different products and use different cleavage mechanisms. *Appl. Environ. Microbiol.* **2014**, *80*, 5012–5020. [[CrossRef](#)] [[PubMed](#)]
81. Fainleib, A.; Pires, R.V.; Lucas, E.F.; Soares, B.G. Degradation of non-vulcanized natural rubber—Renewable resource for fine chemicals used in polymer synthesis. *Polimeros* **2013**, *23*, 441–450. [[CrossRef](#)]
82. Craciun, G.; Manaila, E.; Stelescu, M.D. Materials new elastomeric materials based on natural rubber obtained by electron beam irradiation for food and pharmaceutical use. *Materials* **2018**, *9*, 999. [[CrossRef](#)] [[PubMed](#)]
83. Allan, K.M. The Microbial Devulcanisation of Waste Ground Tyre Rubber Using Acidophilic Microorganisms. Ph.D. Thesis, Stellenbosch University, Stellenbosch, South Africa, March 2018.
84. Kole, P.J.; Löhr, A.J.; Van Belleghem, F.G.A.J.; Ragas, A.M.J. Wear and tear of tyres: A stealthy source of microplastics in the environment. *Int. J. Environ. Res. Public Health* **2017**, *14*, 1265. [[CrossRef](#)] [[PubMed](#)]
85. Sieber, R.; Kaweck, D.; Nowack, B. Dynamic probabilistic material flow analysis of rubber release from tires into the environment. *Environ. Pollut.* **2020**, *258*, 113573. [[CrossRef](#)]